New approaches to explore dark matter and baryogenesis

Fa Peng Huang

Department of Physics and McDonnell Center for the Space Sciences,
Washington University, St. Louis

Particle Physics on the Plains
@ University of Kansas
October 12, 2019

Outline

- ➢Research motivation and background
- ➢Indirect search for pseudo scalar (axion) cold dark matter (DM) by SKA-like experiments
- ➢Indirect search for scalar DM and baryogenesis by LISA-like&CEPC-like experiments.
- ➢Summary and outlook

Motivation

Whenever we see this cosmic pie, we are always confused: what is the nature of DM & the baryon asymmetry of the universe?

A lot of experiments have be done to unravel these long-standing problems.

However, there is no signals of new physics at LHC and dark matter direct search.

This situation may just point us towards new approaches, especially (my personal interest) Radio telescope experiments (SKA, FAST, GBT…) & Laser Interferometer experiments (LISA, Tianqin/Taiji…)

Focus on new approaches to explore two popular (pseudo) scalar DM:axion-like particles and scalar DM in scalar extended model.

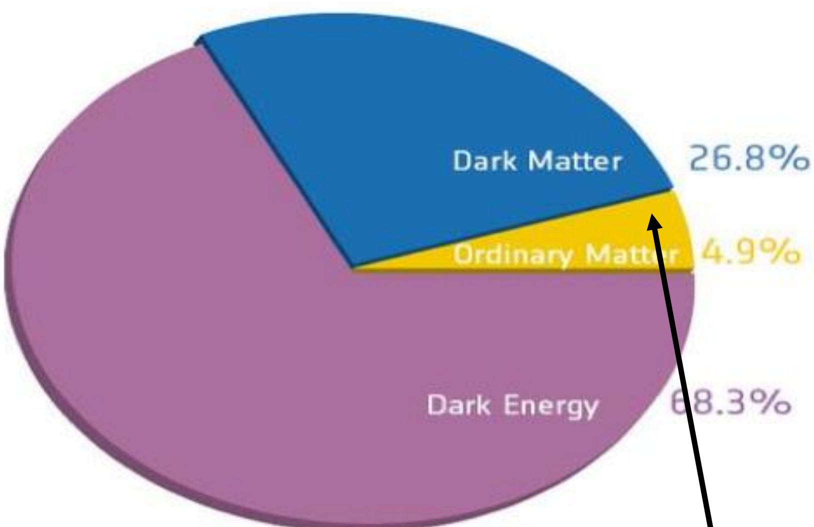

Why negligible antimatter,
(baryon asymmetry of the universe)?

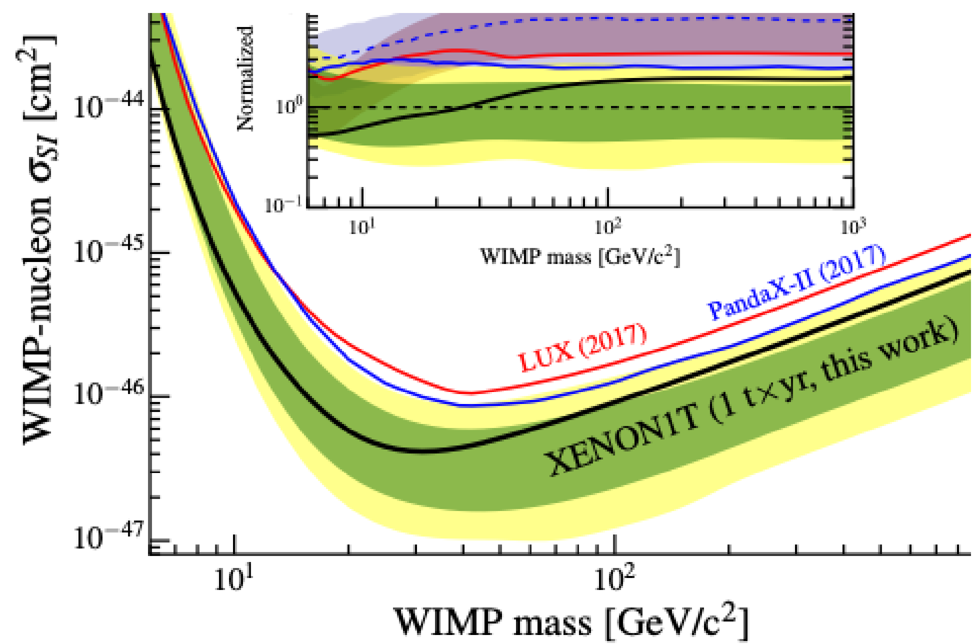

Phys.Rev.Lett. 121 (2018) no.11, 111302

Motivation

Higgs in EW phase transition and baryogenesis: LISA, Tianqin/Taiji

QCD phase transition and **axion** cold DM: SKA, FAST, GBT(radio telescope)

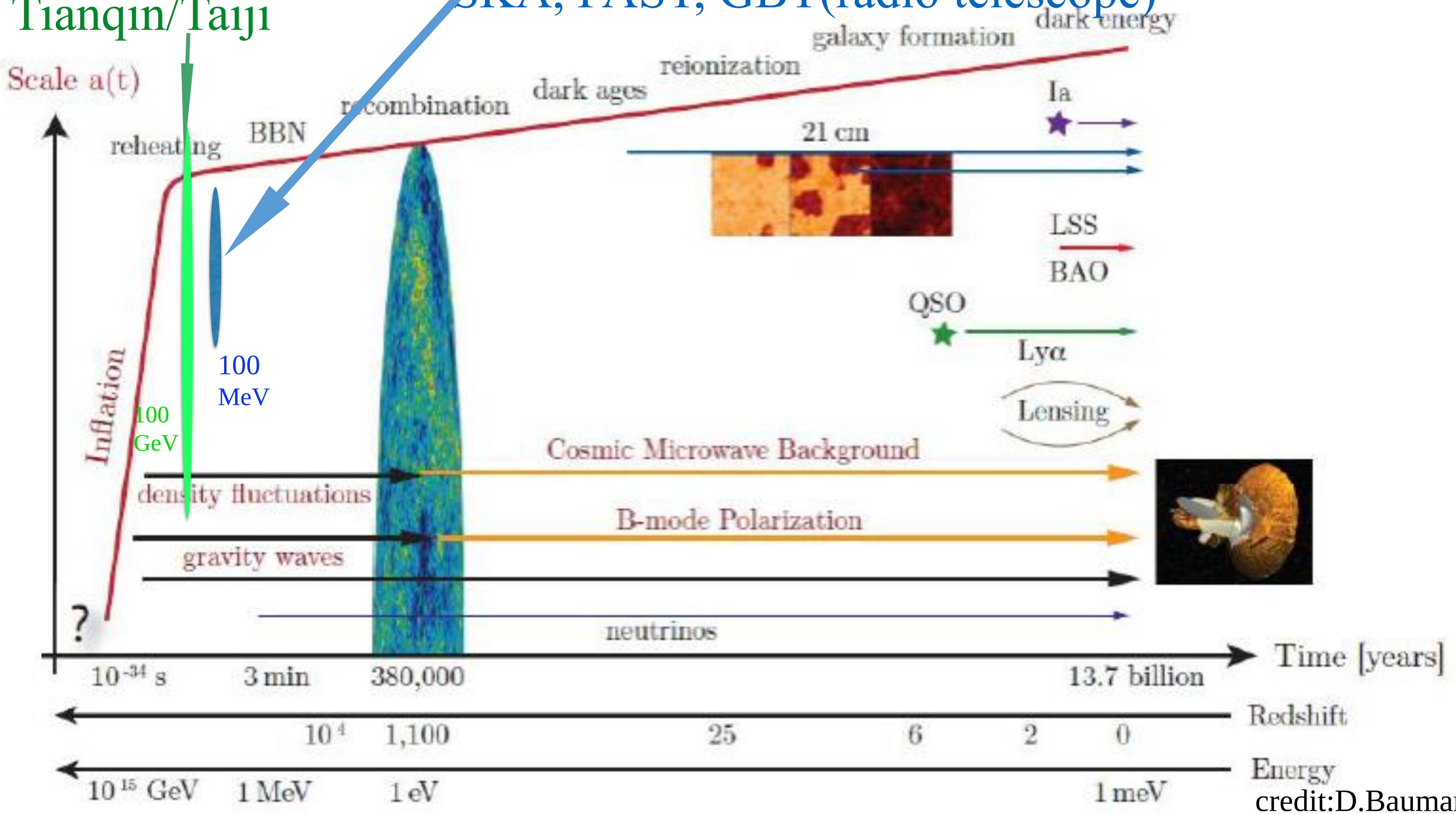

credit:D.Baumann

The Square Kilometre Array (SKA)

Early science observations are expected to start in 2020 with a partial array.

credit: SKA website

The Square Kilometre Array (SKA)

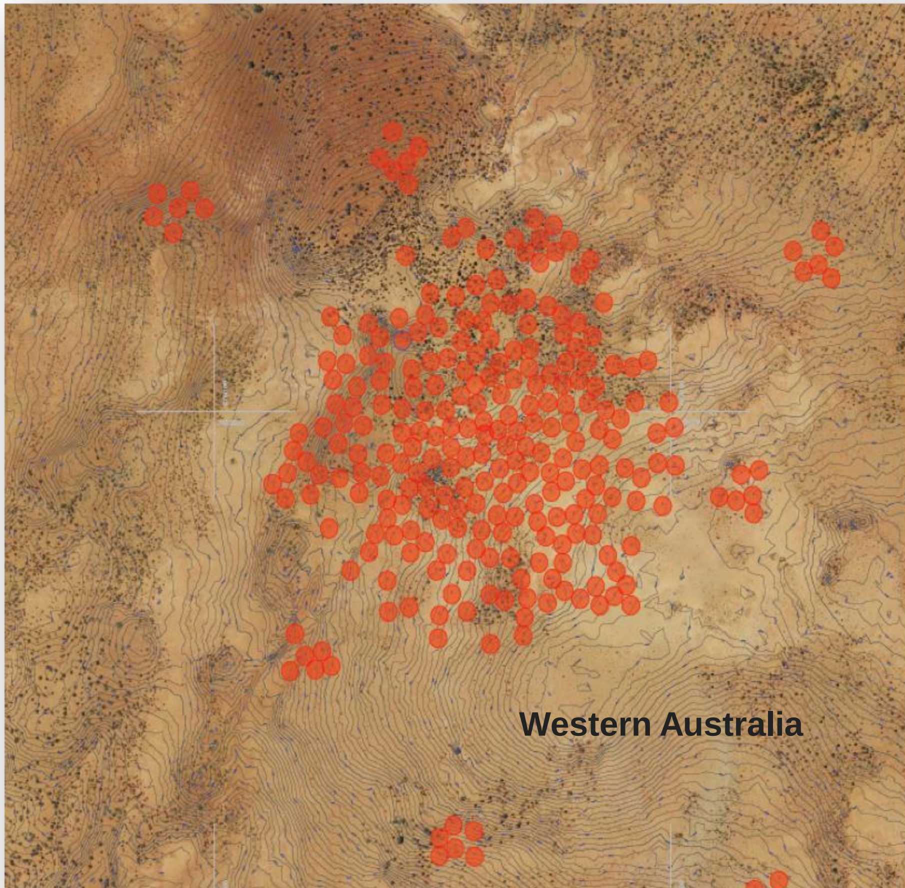

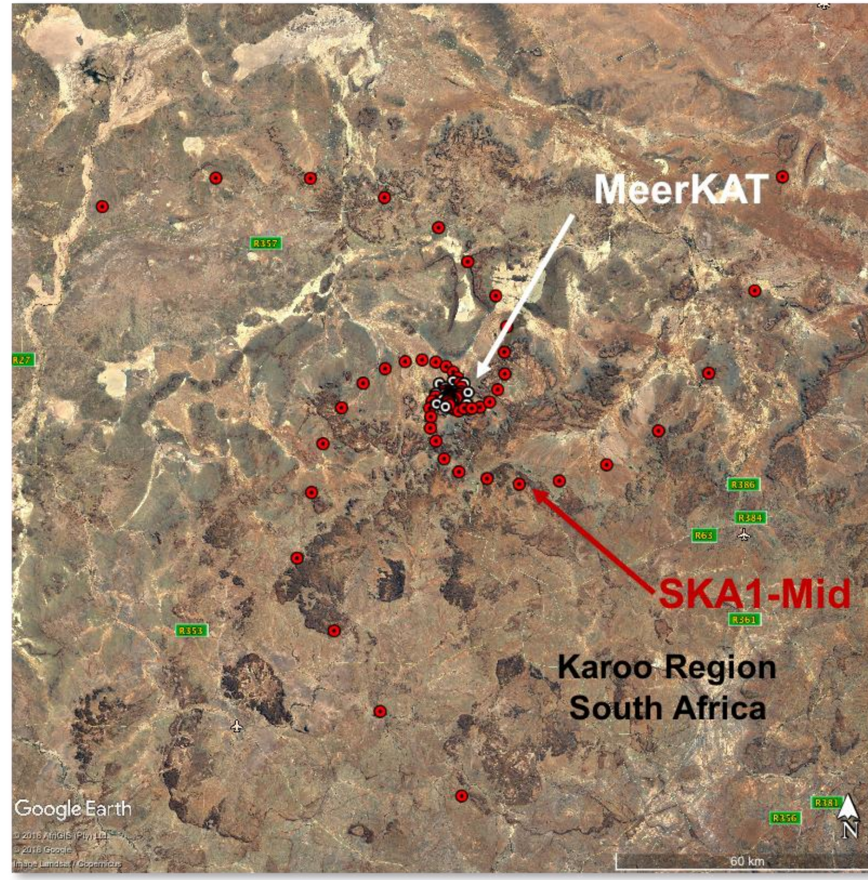

Organisations from 13 countries are members of the SKA Organisation – Australia, Canada, China, France, Germany, India, Italy, New Zealand, Spain, South Africa, Sweden, The Netherlands and the United Kingdom.

Early science observations are expected to start in 2020 with a partial array.

credit: SKA website

Powerful SKA experiments

High sensitivity: SKA surveys will probe to sub-micro-Jy levels.The extremely high sensitivity of the thousands of individual radio receivers, combining to create the world's largest radio telescope will give us insight into many aspects of fundamental physics

- **How do galaxies evolve? What is dark energy?**
- **Strong-field tests of gravity using pulsars and black holes**
- **The origin and evolution of cosmic magnetism**
- **Probing the Cosmic Dawn**
- **The cradle of life**
- **Flexible design to enable exploration of the unknown, such as axion DM**

credit: SKA website

SKA can also helps to explore the evolution history of the universe around 100 MeV, dark matter…

Pulsar timing signal from ultralight scalar DM (probe fuzzy DM by SKA) **JCAP 1402 (2014) 019,A. Khmelnitsky, V. Rubakov**

The Five-hundred-meter Aperture Spherical radio Telescope (FAST)

1112 days in operation since 25th Sep. 2016

Credit:FAST website

The Green Bank Telescope (GBT)

GBT is running observations roughly 6,500 hours each year

credit:GBT website

Laser Interferometer Space Antenna (LISA)

Launch in 2034 or even earlier

credit:LISA website

Powerful LISA experiments

- **Gravitational wave (GW) (Exp: LISA 2034) from compact binary**
- **The true shape of Higgs potential (Exp: complementary test with CEPC)**(FPH,et.al,Phys.Rev. D93 (2016) no.10, 103515， Phys.Rev. D94 (2016) no.4, 041702)
- Baryon **asymmetry of the universe (baryogenesis)**
- **DM blind spots** **Phys.Rev. D98 (2018) no.9, 095022, FPH,Jianghao Yu**
- **Asymmetry DM**

(**The cosmic phase transition with Q-balls production mechanism can explain the baryogenesis and DM simultaneously, where constraints on DM masses and reverse dilution are significantly relaxed.**
FPH, Chong Sheng Li, Phys.Rev. D96 (2017) no.9, 095028)

LISA in synergy with future lepton collider helps to explore the evolution history of the universe at several hundred GeV temperature, DM and baryogenesis.

Complementary of particle and wave experiments

Particle approach

we can build more powerful colliders, such as planned CEPC/SppC, FCC etc.

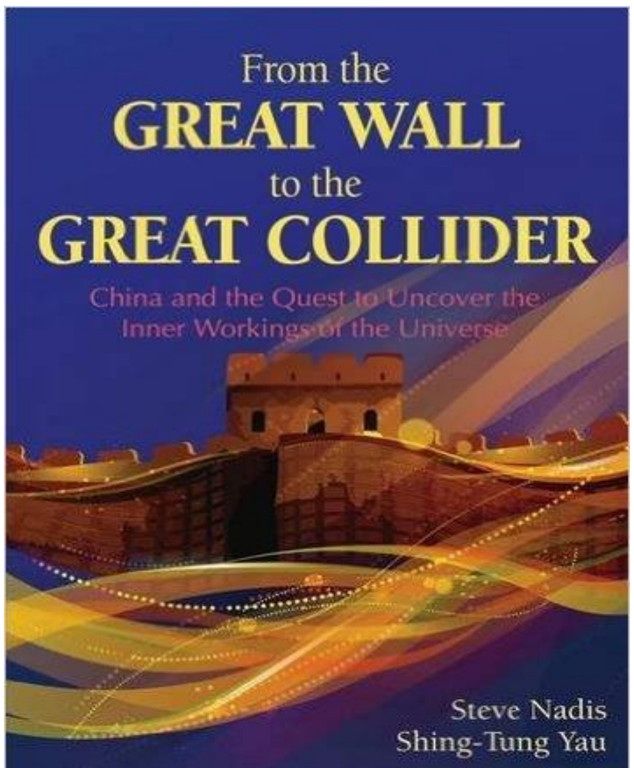

Relate by Higgs physics:EW phasetransition/baryogenesis

Double test on the Higgs potential and baryogenesis, DM

Wave approach

GW detectors can test Higgs potential as complementary approach. (LISA launch 2034)

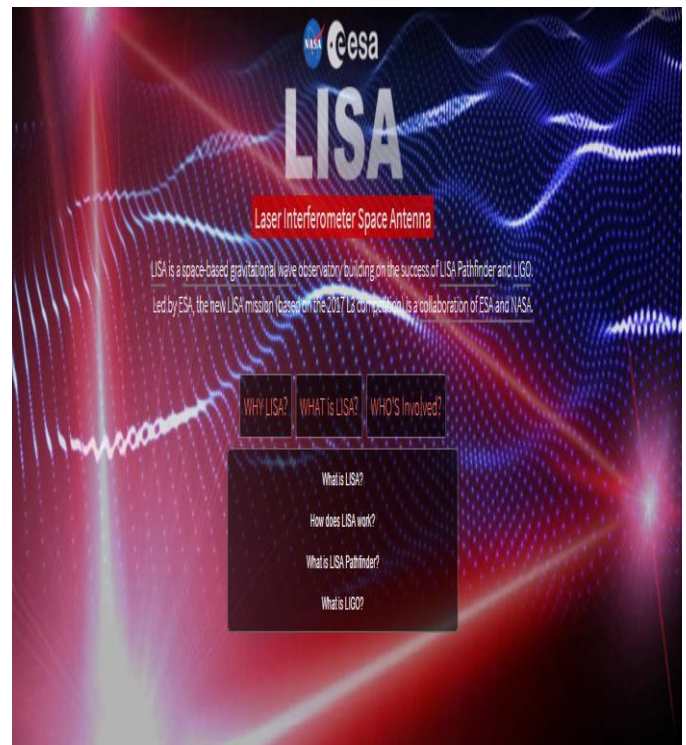

I. Typical pseudo scalar DM: Explore the axion cold dark matter by SKA-like experiments

Axion or axion-like particle motivated from strong CP problem or string theory is still one of the most attractive and promising DM candidate.

We firstly study using the SKA-like experiments to explore the resonant conversion of axion cold DM to radio signal from magnetized astrophysical sources, such as neutron star, magnetar and pulsar.

FPH, K. Kadota, T. Sekiguchi, H. Tashiro, Phys.Rev. D97 (2018) no.12, 123001, arXiv:1803.08230

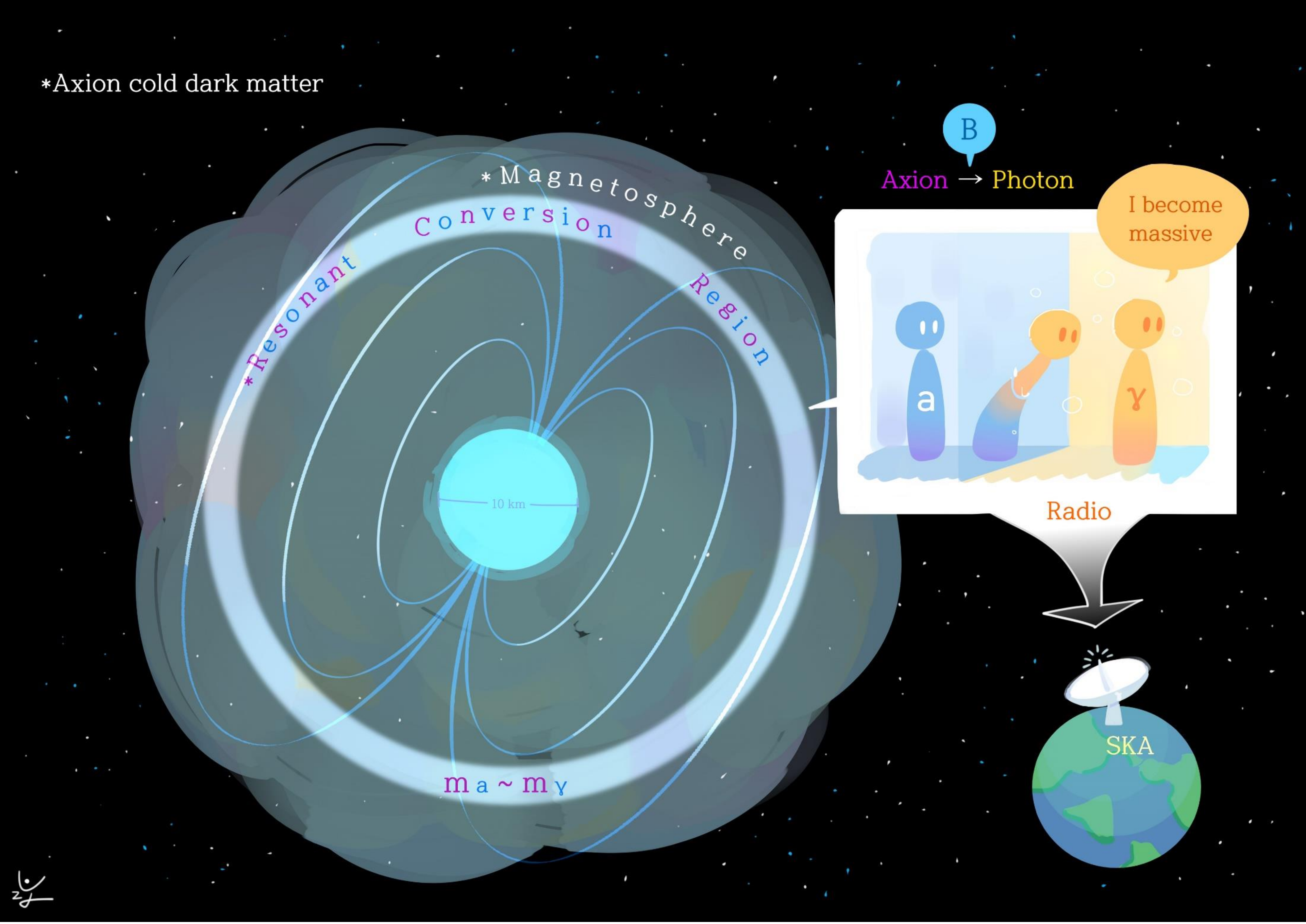

FPH, K. Kadota, T. Sekiguchi, H. Tashiro, Phys.Rev. D97 (2018) no.12, 123001

Radio telescope search for the resonant conversion of cold DM axions from the magnetized astrophysical sources

Three key points:

- ➢**Cold DM is composed of non-relativistic axion or axion-like particles, and can be accreted around the neutron star**
- ➢**Neutron star (or pulsar and magnetar) has the strongest position-dependent magnetic field in the universe**
- ➢**Neutron star is covered by magnetosphere and photon becomes massive in the magnetosphere**

Quick sketch of the neutron star size

Radius of neutron star is slightly larger than radius of the LHC circle.

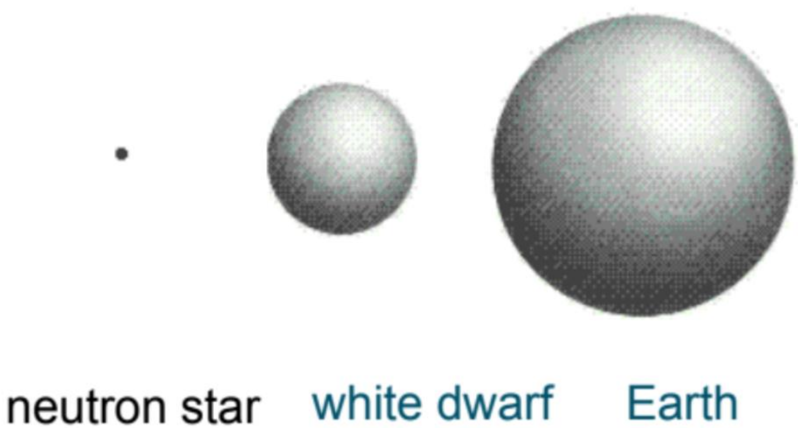

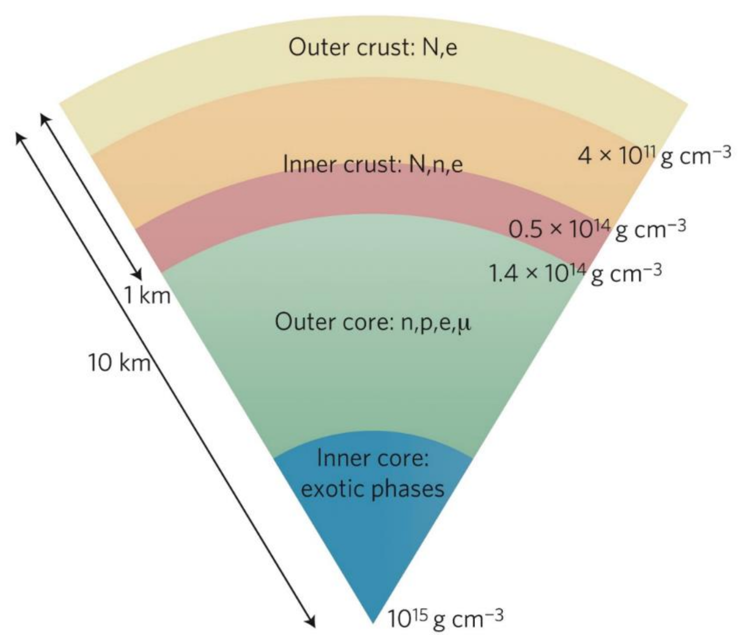

Strong magnetic field in the magnetosphere of Neutron star, Pulsar, Magnetar: the strongest magnetic field in the Universe

1.Mass: from 1 to 2 solar mass, recently GBT find a neutron star with 2 solar mass.

2. Radius: $r_0 \sim 10 - 20\text{km}$

The typical diameter of neutron star is just half-Marathon.

3. Strongest magnetic field at the surface of the neutron star

$$B_0 \approx 10^{12} - 10^{15}\text{G}$$

$$B_0 \sim 3.3 \times 10^{19} \sqrt{P\dot{P}} \quad \text{G}$$

P is the period of neutron star

4. Neutron star is surrounded by large region of magnetosphere, where photon becomes massive.

Alfven $r \sim 100 r_0$

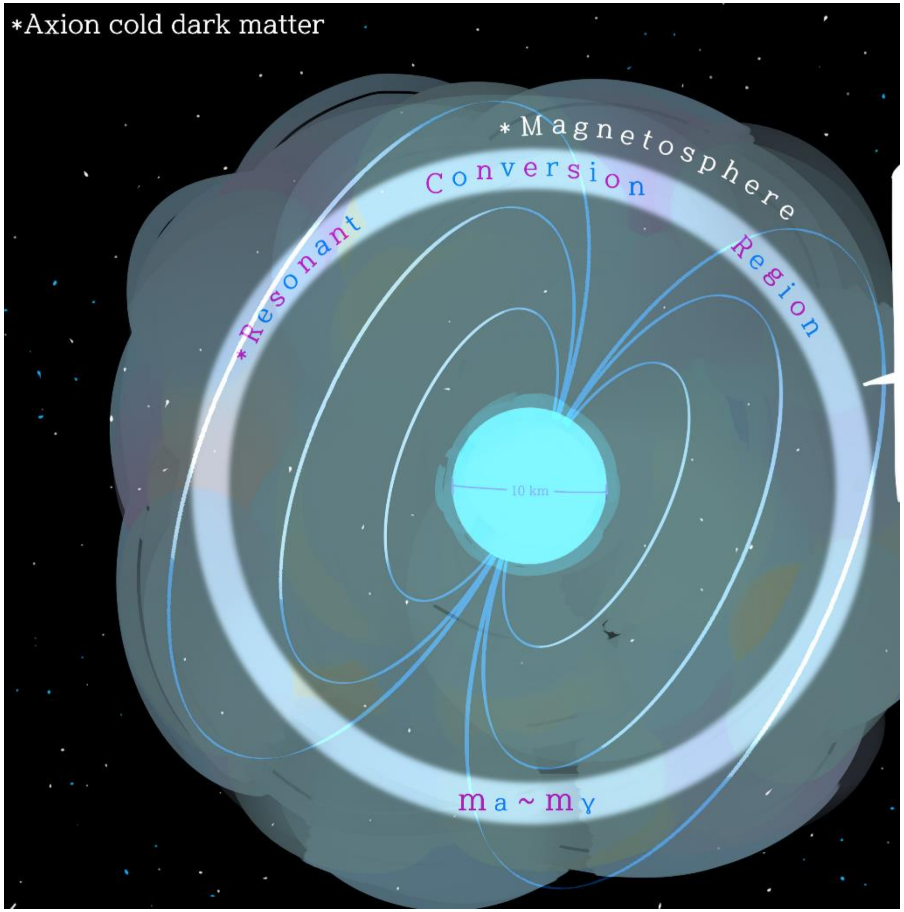

Axion-photon conversion in magnetosphere

The Lagrangian for axion-photon conversion the magnetosphere

$$L = -\frac{1}{4}F_{\mu\nu}F^{\mu\nu} + \frac{1}{2}(\partial_\mu a \partial^\mu a - m_a^2 a^2) + L_{\rm int} + L_{\rm QED}$$

Massive Photon: In the magnetosphere of the neutron star, photon obtains the effective mass in the magnetized plasma.

$$L_{\rm QED} = \frac{\alpha^2}{90 m_e^4}\frac{7}{4}(F_{\mu\nu}\tilde{F}^{\mu\nu})^2 \; +\ldots$$

$$m_\gamma^2 = Q_{\rm pl} - Q_{\rm QED}$$

$$Q_{\rm QED} = \frac{7\alpha}{45\pi}\omega^2\frac{B^2}{B_{\rm crit}^2}$$

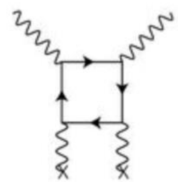

$$Q_{\rm plasma} = \omega_{\rm plasma}^2 = 4\pi\alpha\frac{n_e}{m_e}$$

$$\frac{Q_{\rm pl}}{Q_{\rm QED}} \sim 5\times 10^8\left(\frac{\mu{\rm eV}}{\omega}\right)^2\frac{10^{12}\ {\rm G}}{B}\frac{1\ {\rm sec}}{P}$$

For relativistic axion from neutron star, QED mass dominates and there is no resonant conversion.

$$L_{\rm int} = \frac{1}{4}g\tilde{F}^{\mu\nu}F_{\mu\nu}a = -g\mathbf{E}\cdot\mathbf{B}a,$$

Axion-photon conversion in external magnetic field

G. Raffelt and L. Stodolsky, Phys. Rev. D 37, 1237 (1988)

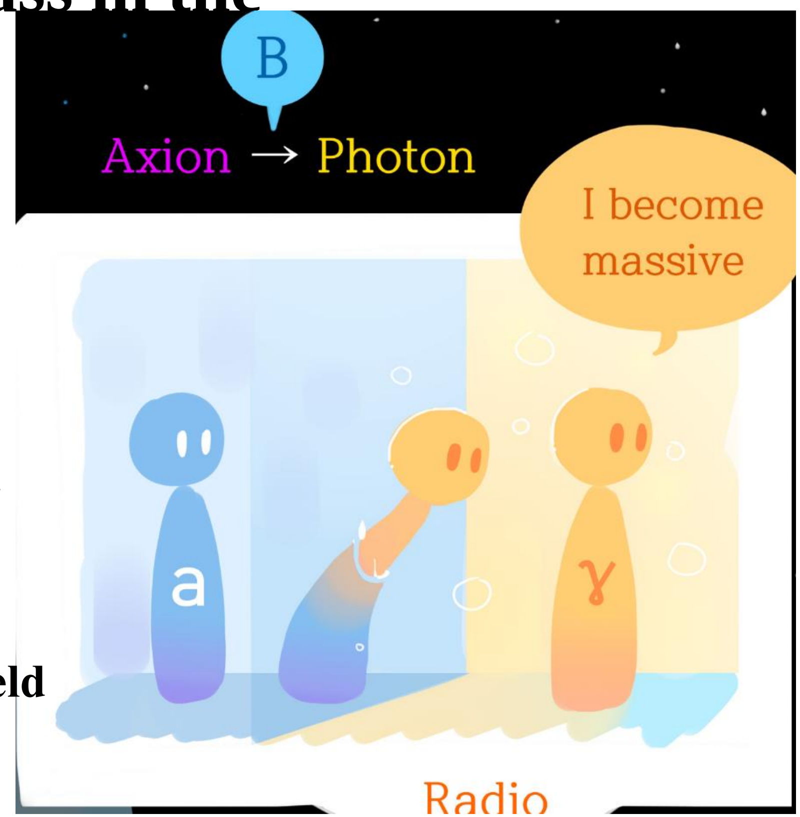

Axion-photon conversion in magnetosphere

The axion-photon conversion probability

$$p_{a\to\gamma} = \sin^2 2\tilde{\theta}(z)\sin^2[z(k_1 - k_2)/2]$$

$$\sin 2\tilde{\theta} = \frac{2gB\omega}{\sqrt{4g^2B^2\omega^2 + (m_\gamma^2 - m_a^2)^2}}$$

$$m_\gamma^2(r) = 4\pi\alpha\frac{n_e(r)}{m_e}$$

Here, for non-relativistic axion cold dark matter, the QED mass is negligible compared to plasma mass.

$$n_e(r) = n_e^{\mathrm{GJ}}(r) = 7\times 10^{-2}\frac{1s}{P}\frac{B(r)}{1\ \mathrm{G}}\frac{1}{\mathrm{cm}^3} \qquad B(r) = B_0\left(\frac{r}{r_0}\right)^{-3}$$

Here, we choose the simplest electron density distribution and magnetic field configuration to clearly see the physics process.

Thus, the photon mass is position r dependent, and within some region the photon mass is close to the axion DM mass.

The Adiabatic Resonant Conversion
Of Axion into photon

The resonance radius is defined at the level crossing point

$$m_\gamma^2(r_{\rm res}) = m_a^2$$

At the resonance, $|m_\gamma^2 - m_a^2| \ll gB\omega$ and $m_{1,2}^2 \approx m_a^2 \pm gB\omega$.

Within the resonance region, the axion-photon conversion rate is greatly enhanced due to large mixing angle.

$$\sin 2\tilde{\theta} = \frac{(2gB\omega/m_\gamma^2)}{\sqrt{(4g^2B^2\omega^2/m_\gamma^4) + (1-(m_a/m_\gamma)^2)^2}} \equiv \frac{c_1}{\sqrt{c_1^2 + (1-f(r))^2}},$$

N.B. Only for the non-relativistic axion, the resonant conversion can be achieved. For relativistic axion, QED effects make it impossible.

The adiabatic resonant conversion requires the resonance region is approximately valid inside the resonance width. Coherent condition is also needed.

$$\delta r > l_{\rm osc} = \frac{2\pi}{|k_1 - k_2|_{\rm res}}$$

$$|d\tilde{\theta}/dr|_{\rm res} < l_{\rm osc}^{-1}$$

$$|d\ln f/dr|_{\rm res}^{-1} > 650[m]\left(\frac{m_a}{\mu\mathrm{eV}}\right)^3\left(\frac{v_{\rm res}}{10^{-1}}\right)\left(\frac{1/10^{10}\ \mathrm{GeV}}{g}\right)^2 \times\left(\frac{10^{12}\ \mathrm{G}}{B(r_{\rm res})}\right)^2\left(\frac{\mu\mathrm{eV}}{\omega}\right)^2$$

Adiabatic resonant conversion is essential to observe the photon signal.

Radio Signal

Line-like radio signal for non-relativistic axion conversion:

$$\nu_{\rm peak} \approx \frac{m_a}{2\pi} \approx 240 \frac{m_a}{\mu eV} \text{MHz}$$

1 GHz ~ 4 μeV

The FAST covers 70 MHz–3 GHz, the SKA covers 50 MHz–14 GHz, and the GBT covers 0.3–100 GHz, so that the radio telescopes can probe axion mass range of 0.2–400 μeV

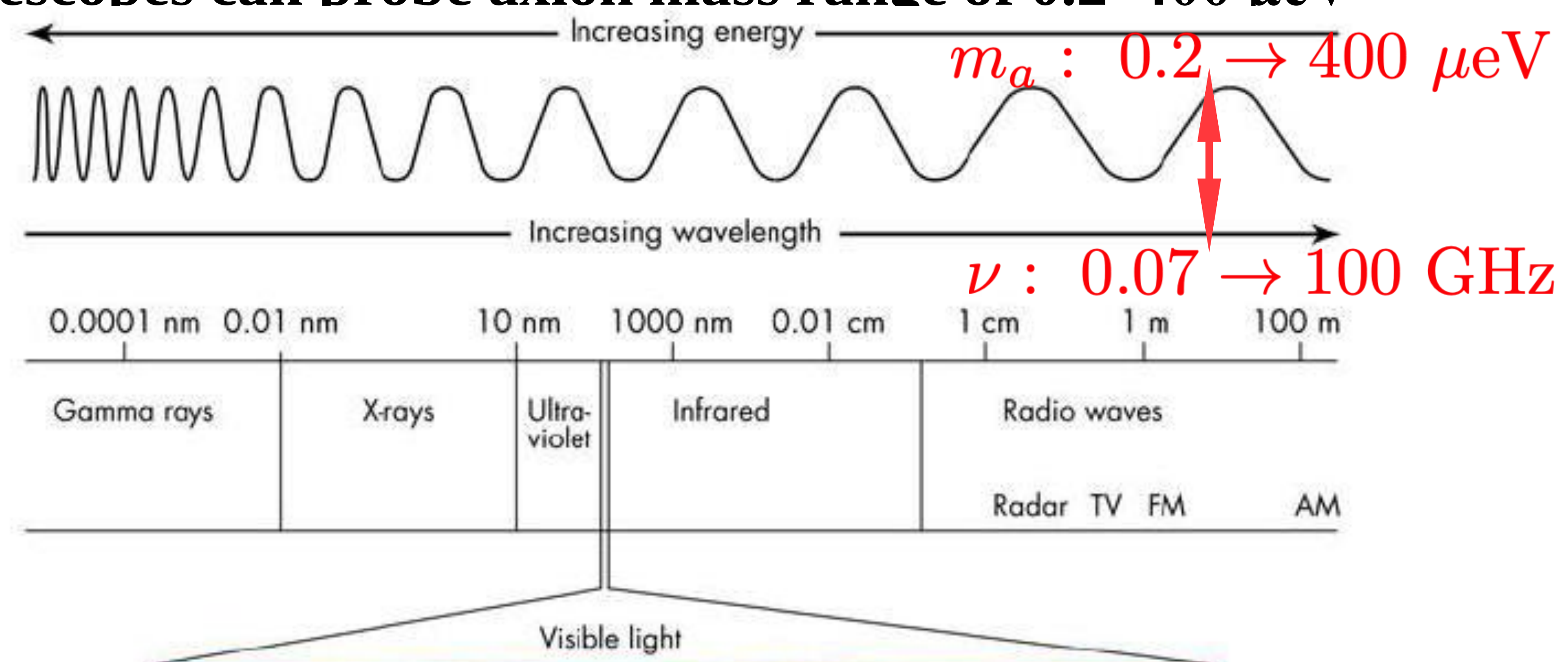

Radio Signal

Signal: For adiabatic resonant conversion, and the photon flux density can be estimated to be of order

$$S_\gamma = \frac{dE/dt}{4\pi d^2 \Delta\nu} \sim 4.2\mu Jy \frac{\left(\frac{r_{\rm res}}{100\ {\rm km}}\right)\left(\frac{M}{M_{\rm sun}}\right)\left(\frac{\rho_a}{0.3\ {\rm GeV/cm^3}}\right)\left(\frac{10^{-3}}{v_0}\right)\left(\frac{g}{1/10^{10}\ {\rm GeV}}\right)\left(\frac{B(r_{\rm res})}{10^{12}\ {\rm G}}\right)\left(\frac{\omega}{\mu{\rm eV}}\right)\left(\frac{\mu{\rm eV}}{m_a}\right)^2}{\left(\frac{d}{1\ {\rm kpc}}\right)^2\left(\frac{m_a/2\pi}{\mu{\rm eV}/2\pi}\right)\left(\frac{v_{\rm dis}}{10^{-3}}\right)},$$

where d represents the distance from the neutron star to us. The photon flux peaks around the frequency $\nu_{\rm peak} \sim m_a/2\pi$, and $\Delta\nu \sim \nu_{\rm peak} v_{\rm dis}$ represents the spectral line broadening around this peak frequency due to the DM velocity dispersion $v_{\rm dis}$.

Sensitivity: The smallest detectable flux density of the radio telescope (SKA, FAST, GBT) is of order

$$S_{\rm min} \approx 0.29\mu Jy \left(\frac{1\ {\rm GHz}}{\Delta B}\right)^{1/2}\left(\frac{24\ {\rm hrs}}{t_{\rm obs}}\right)^{1/2}\left(\frac{10^3\ {\rm m^2/K}}{A_{\rm eff}/T_{\rm sys}}\right)$$

Radio Signal

Signal: For a trial parameter set, $B_0 = 10^{15}$ G, $m_a = 50\ \mu$eV

$P = 10$ s, $g = 5 \times 10^{-11}$ GeV^{-1}, $r_0 = 10$ km, $M = 1.5 M_{\rm sun}$, $d = 1$kpc

satisfies the constraints of the adiabatic resonance conditions and the existed axion search constraints produces the signal S$_\gamma$~0.51 μJy.

Sensitivity: $S_{\min} \sim 0.48 \mu Jy$ for the SKA1

$S_{\min} \sim 0.016 \mu Jy$ for the SKA2 with 100 hour observation time

SKA-like experiment can probe the axion DM and the axion mass which corresponds to peak frequency.

More detailed study taking into account astrophysical uncertainties and more precise numerical analysis is still working in progress.

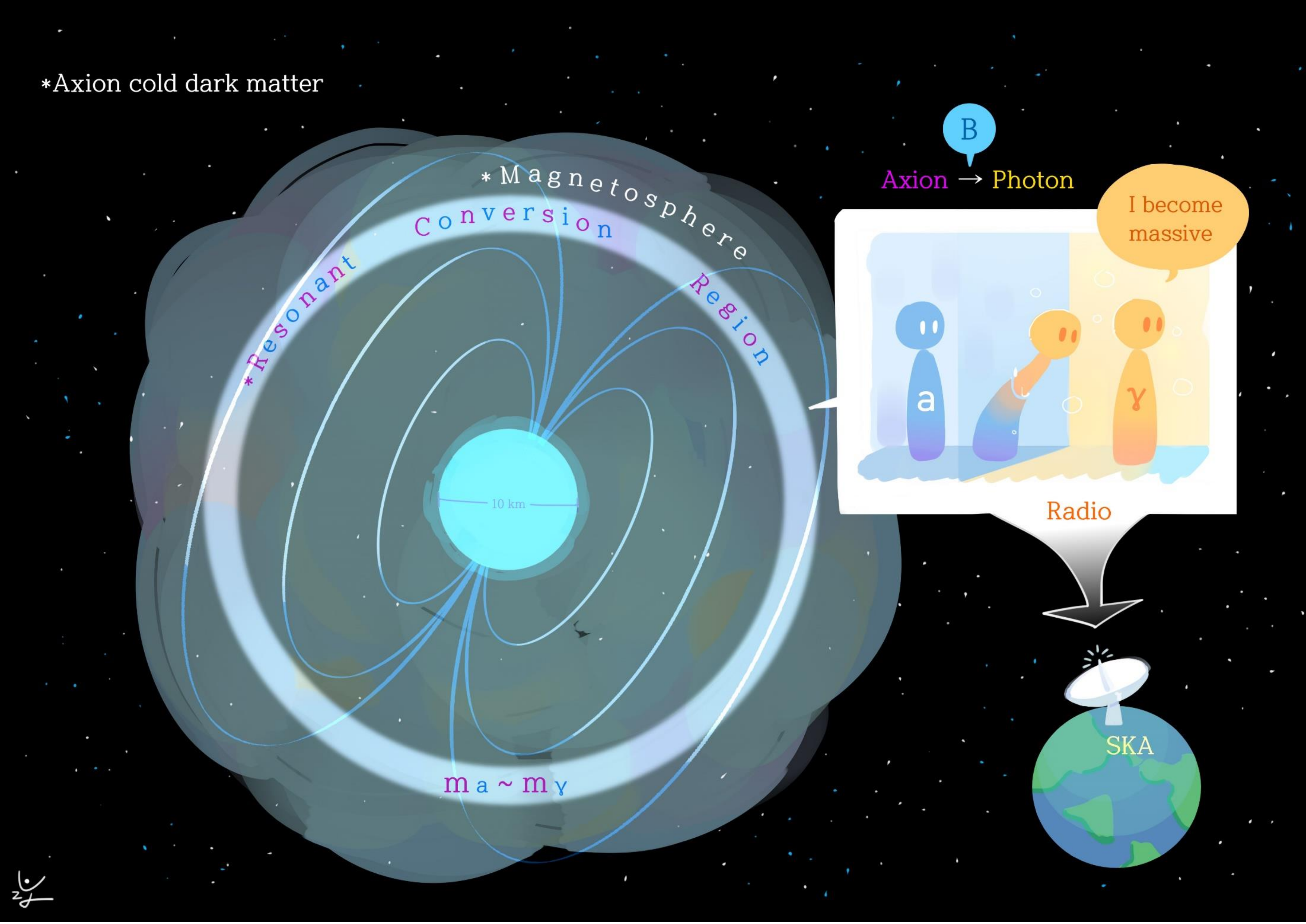

FPH, **K. Kadota, T. Sekiguchi, H. Tashiro, Phys.Rev. D97 (2018) no.12, 123001**

Comments on the radio probe of axion dark DM

1. Astrophysical uncertainties:the magnetic profile, DM density and distribution, the velocity dispersion, the plasma mass, background including optimized bandwidth

2. There are more and more detailed and comprehensive studies after our first rough estimation on the radio signal:

arXiv:1804.03145 by Anson Hook, Yonatan Kahn, Benjamin R. Safdi, Zhiquan Sun where they consider more details. They also consider extremely high DM density around the neutron star, thus the signal is more stronger.

arXiv:1811.01020 by Benjamin R. Safdi, Zhiquan Sun, Alexander Y. Chen

arXiv:1905.04686,Thomas, D.P.Edwards,M. Chianese, B. J. Kavanagh, S. M. Nissanke, C. Weniger, where they consider multi-messenger of axion DM detection. Namely, using LISA to detect the DM density around the neutron star, which can determine the radio strength detected by SKA.

3. Recently, GBT already have some data on the observation of neutron star, and Safdi’s group is doing the analysis of the data to get some constraints.

4. More precise study are needed …

Comments on the radio probe of axion DM

arXiv:1804.03145 by Anson Hook, Yonatan Kahn, Benjamin R. Safdi, Zhiquan Sun where they consider more details.
Besides the normal DM density, they also consider the extremely high DM density around the neutron star, thus the signal is more stronger.

arXiv:1811.01020 by Benjamin R. Safdi, Zhiquan Sun, Alexander Y. Chen

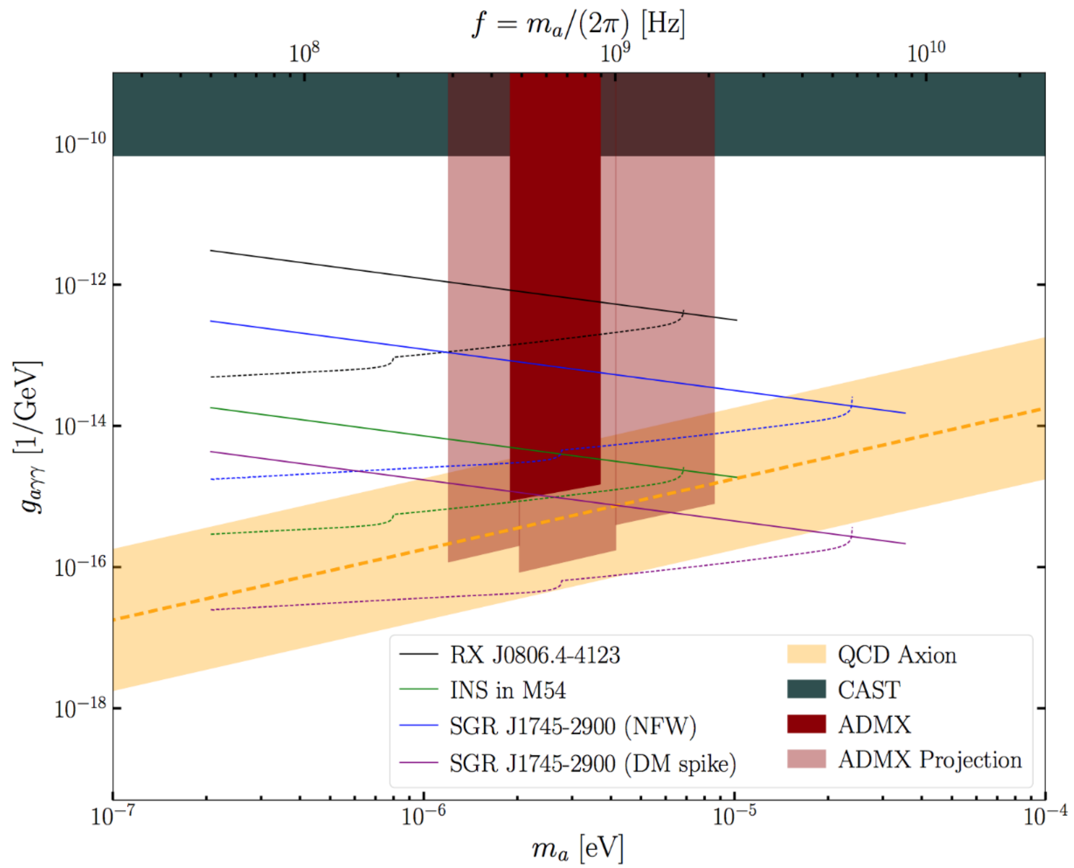

Multi-Messenger Signal of QCD Axion DM

arXiv:1905.04686,Thomas, D.P.Edwards,Marco Chianese, Bradley J. Kavanagh,
Samaya M. Nissanke, Christoph Weniger

How can we use next generation gravitational wave and radio telescopes to find DM?

This work is a combination of two classes of well-studied works:

1. **radio signal search of the axion DM by SKA-like experiments**

3. **gravitational wave detection of DM density by LISA-like experiments.**

These two different works are combined as multi-messenger signals through the extremely high DM density surrounded the intermediate massive black hole and neutron star binary.

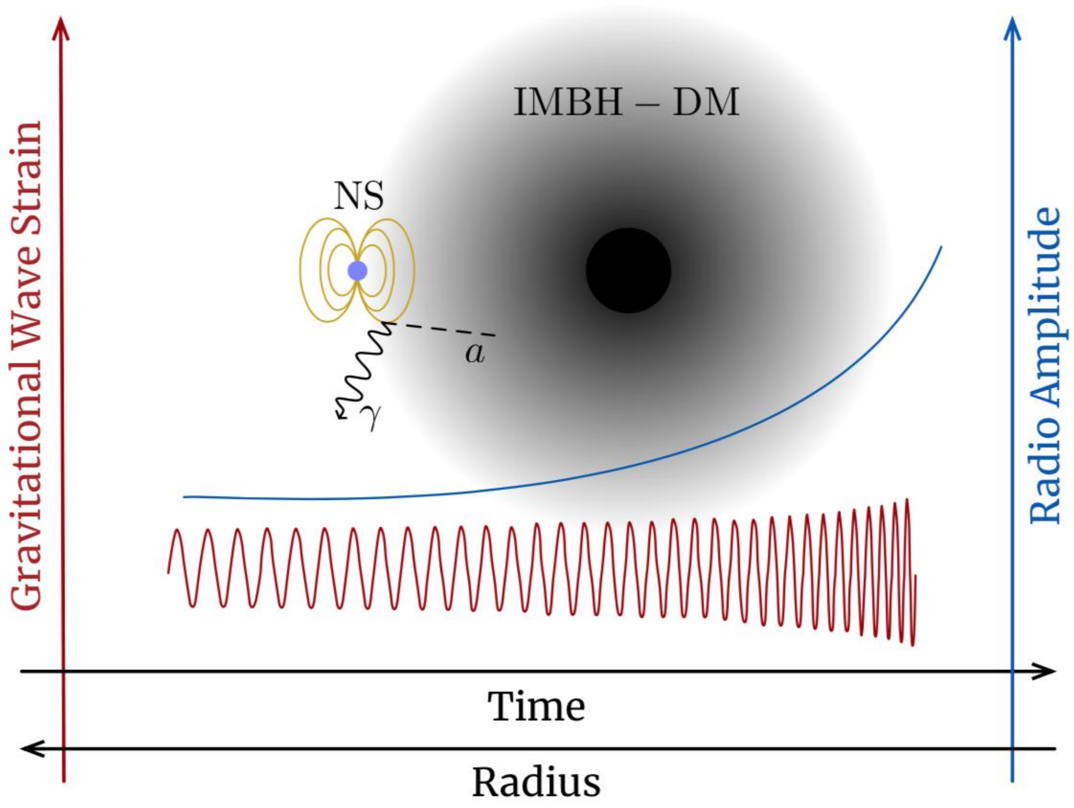

FIG. 1. **Illustration of the IMBH-DM-NS system.** The presence of an axion DM halo around the intermediate mass black hole (IMBH) produces a phase shift in the strain of the GW signal and radio emission due to its conversion into photons in the neutron star (NS) magnetosphere. a and γ represent an axion and radio photon respectively.

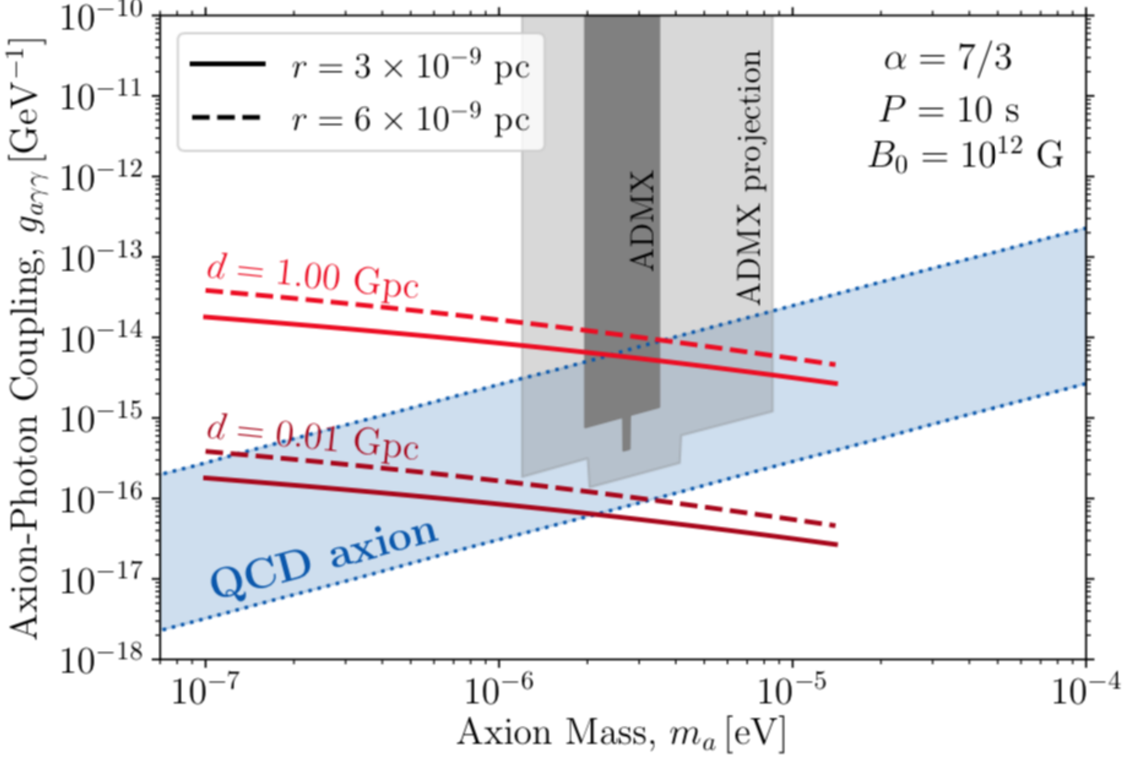

FIG. 3. **Projected sensitivity to the axion-photon coupling from radio observations.** Sensitivity curves of the SKA telescope (100 hours of observation) to the axion-photon coupling as a function of the axion mass for two different inspiral orbits, $r = 6 \times 10^{-9}$ pc (dashed) and $r = 3 \times 10^{-9}$ pc (solid), and two different IMBH-DM-NS system locations, $d = 0.01$ Gpc (dark red) and $d = 1.00$ Gpc (light red). Here, we assume $\alpha = 7/3$ for the slope of the DM spike. The predicted range of parameters for the QCD axion are represented by the blue band, while the vertical gray bands show the current and future ADMX limits [22, 23].

Generalisation to dark photon DM case

arXiv:1910.xxxxx by Haipeng An, FPH, Jia Liu, and Wei Xue

Recently, people realise that light dark photon can be a promising DM candidate.
We study how to detect this dark photon DM by radio telescope, like SKA following the same idea as the axion DM case.
We can obtain the strongest constraints.

P. W. Graham, J. Mardon and S. Rajendran, Phys. Rev. D **93**, no. 10, 103520 (2016) doi:10.1103/PhysRevD.93.103520 [arXiv:1504.02102 [hep-ph]].

R. T. Co, A. Pierce, Z. Zhang and Y. Zhao, Phys. Rev. D **99**, no. 7, 075002 (2019) doi:10.1103/PhysRevD.99.075002 [arXiv:1810.07196 [hep-ph]].

P. Agrawal, N. Kitajima, M. Reece, T. Sekiguchi and F. Takahashi, arXiv:1810.07188 [hep-ph].

A. J. Long and L. T. Wang, Phys. Rev. D **99**, no. 6, 063529 (2019) doi:10.1103/PhysRevD.99.063529 [arXiv:1901.03312 [hep-ph]].

Generalisation to dark photon DM case

arXiv:1910.xxxxx by Haipeng An, FPH, Jia Liu, and Wei Xue

$$\kappa F'_{\mu\nu} F_{\mu\nu}/2.$$

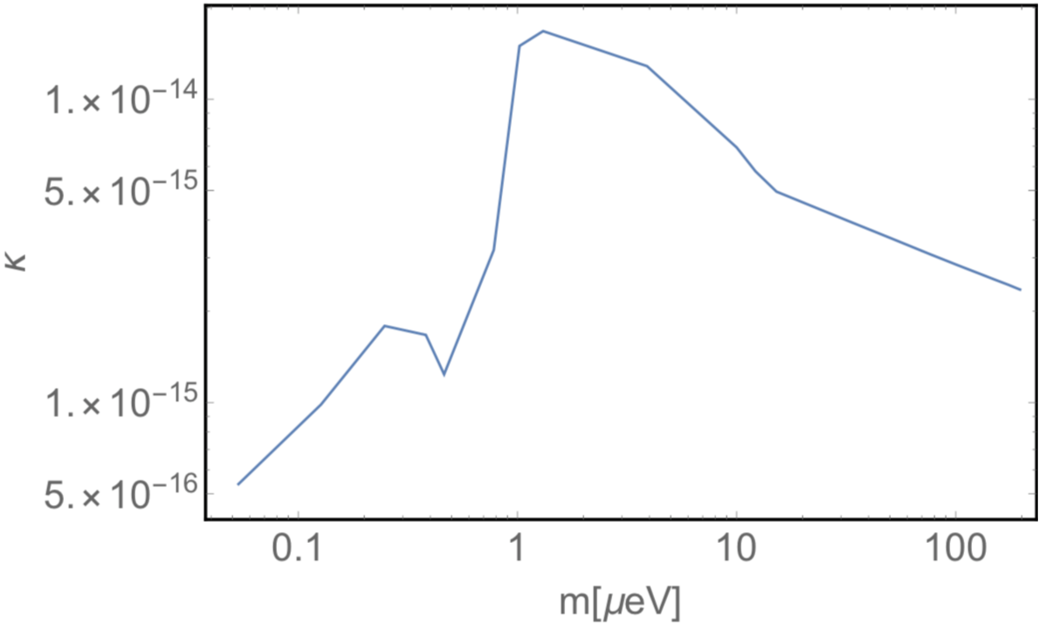

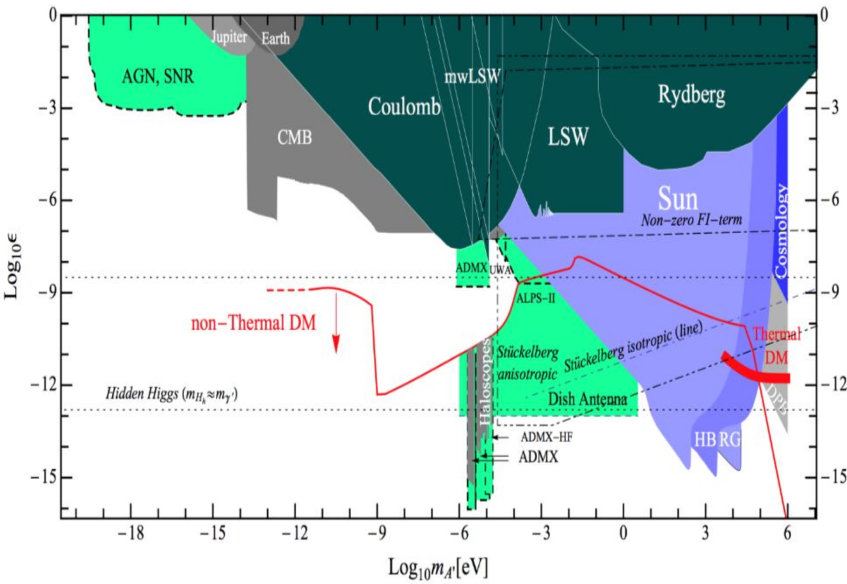

Preliminary constraints from SKA phase 1

II.Typical scalar DM: Explore scalar DM and baryogenesis

We study a simple model for the successful DM and EW baryogenesis with dynamical CP-violating source.

Based on arXiv:1905.10283, FPH, Eibun Senaha

and work in progress with Eibun Senaha 1908.xxxxx

$$V_0(\Phi,\eta) = \mu_1^2\Phi^\dagger\Phi + \mu_2^2\eta^\dagger\eta + \frac{\lambda_1}{2}(\Phi^\dagger\Phi)^2 + \frac{\lambda_2}{2}(\eta^\dagger\eta)^2 + \lambda_3(\Phi^\dagger\Phi)(\eta^\dagger\eta) + \lambda_4(\Phi^\dagger\eta)(\eta^\dagger\Phi) + \left[\frac{\lambda_5}{2}(\Phi^\dagger\eta)^2 + \text{h.c}\right],$$

The new lepton Yukawa interaction is

$$-\mathcal{L}_Y \ni y_{ij}\bar{\ell}_{iL}\eta E_{jR} + m_{E_i}\bar{E}_{iL}E_{iR} + \text{h.c.}$$

vector-like lepton (E_i)

D. Borah, S. Sadhukhan and S. Sahoo, Phys. Lett. B **771**, 624 (2017).
L. Calibbi, R. Ziegler and J. Zupan, JHEP **1807**, 046 (2018).
D. Borah, P. S. B. Dev and A. Kumar, Phys. Rev. D **99**, no. 5, 055012 (2019).

EW baryogenesis and phase transition GW in a nutshell

A long standing problem in particle cosmology is to unravel the origin of baryon asymmetry of the universe (BAU).

After the discovery of the 125 GeV Higgs boson, electroweak (EW) baryogenesis becomes a timely and testable scenario for explaining the BAU.

$\eta = n_B/n_\gamma = 6.05(7) \times 10^{-10}$ **(from CMB, BBN)**

EW baryogenesis

SM technically has all the three elements for baryogenesis , (B aryon violation, C and CP violation, D eparture from thermal equilibrium or CPT violation) but not enough.

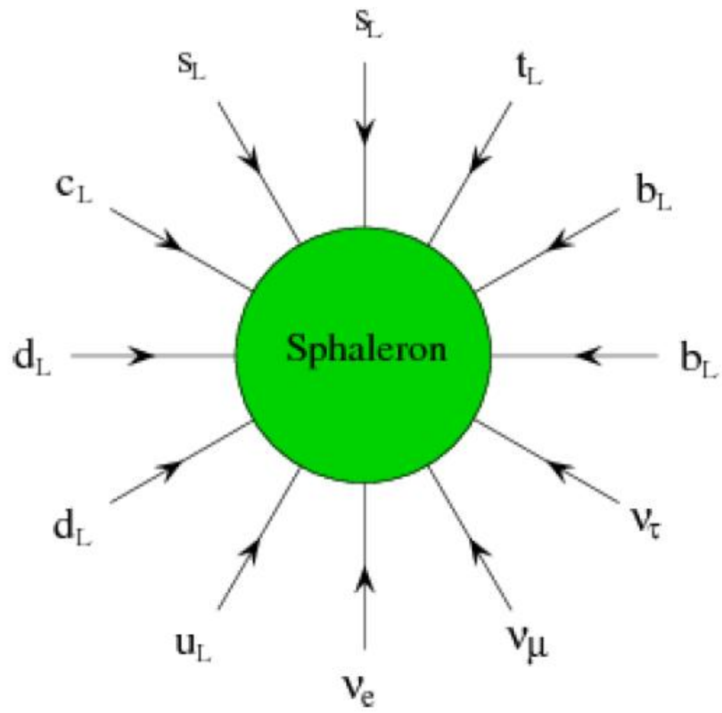

- **B violation from anomaly in B+L current.**
- **CKM matrix, but too weak.**
- **Strong First order phase transition with expanding Higgs Bubble wall.**

From D. E. Morrissey and M. J. Ramsey-Musolf, New J. Phys. 14, 125003 (2012).

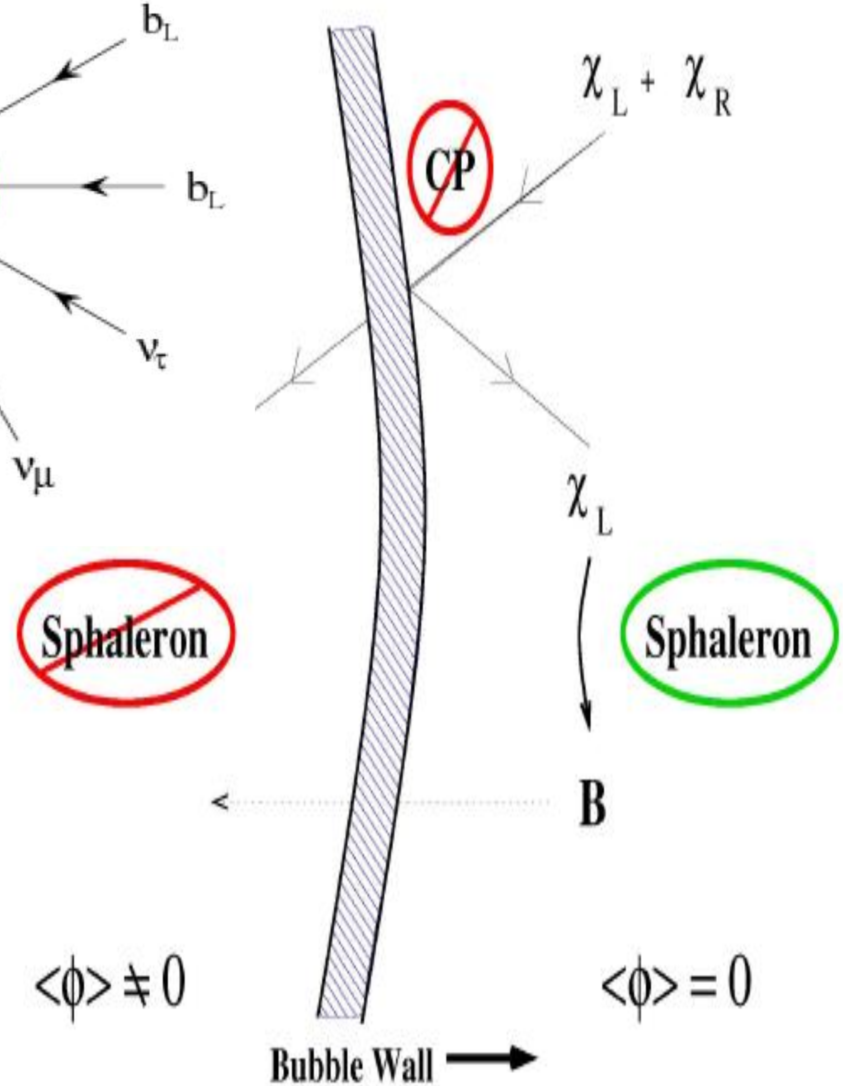

phase transition GWs in a nutshell

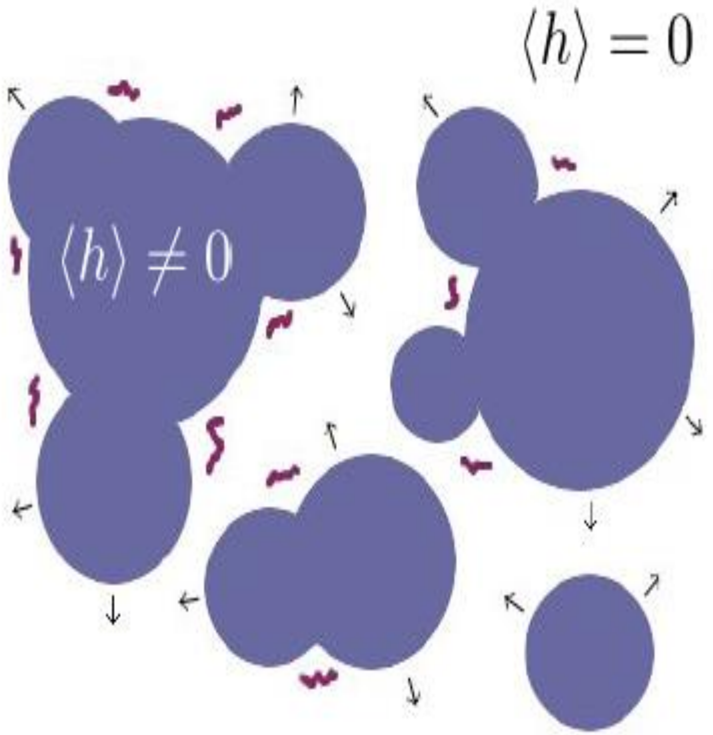

E. Witten, Phys. Rev. D 30, 272 (1984)
C. J. Hogan, Phys. Lett. B 133, 172 (1983);
M. Kamionkowski, A. Kosowsky and M. S. Turner, Phys. Rev. D 49, 2837 (1994))
EW phase transition GWs becomes more interesting and realistic after the discovery of Higgs by LHC and GW by LIGO.

First order phase transition can drive the plasma of the early universe out of thermal equilibrium, and bubble nucleate during it, which will produce GWs.

Pictures from Prof. Huber and Konstandin

Mechanisms of GWs during phase transition

- **Bubble collision:** **well-known source**
- **Turbulence in the plasma fluid:** **a fraction of the bubble wall energy converted into turbulence.**
- **Sound wave in the plasma fluid** **: after the collision a fraction of bubble wall energy converted into motion of the fluid (and is only later dissipated).**

New mechanism of GWs： sound wave
M.Hindmarsh, *et al*., PRL **112**, 041301 (2014);
G. Christophe *et al.* Phys.Rev. D75 (2007)
Caprini, Chiara *et al.* JCAP 1604 (2016)

Detectable GWs signals will be produced during the phase transition from the three mechanisms

Successful DM and EW baryogenesis with dynamical CP-violating source

Current EDM data put severe constraints on many baryogenesis models. For example, ACME Collaboration's new result, i.e.

$|d_e| < 1.1\times 10^{-29}$ **cm · e at 90% C.L.** (Nature vol.562,357,18th Oct.2018) ,

has ruled out a large portion of the CP-violating parameter space for many baryogenesis models.

$|d_e| < 8.7 \times 10^{-29}$ cm · e **(ACME 2014)**

$|d_e| \sim< 1 \times 10^{-29}$ **(ACME 2018)**

Strong tension in most cases

Large enough CP-violating source for successful EW baryogenesis ⟷ **pretty small CP-violation to avoid strong EDM constraints**

How to alleviate this tension for successful EW baryogenesis?

Question: How to alleviate the tension between sufficient CP violation for successful electroweak baryogenesis and strong constraints from current EDM measurements ?

Answer: Dynamical the CP-violating source

Large enough CP-violating source in the early universe for successful EW baryogenesis

Alleviate by assuming the CP-violating source is time dependent

Dynamical/cosmological evolve

Negligible CP-violating source at current time to avoid strong EDM constraints

Complex 2HDM: Xiao Wang, FPH, Xinmin Zhang, arXiv: 1909.02978,
Model independent study: FPH, Zhuoni Qian, Mengchao Zhang,Phys.Rev. D98 (2018) no.1, 015014
FPH,Chong Sheng Li, Phys. Rev. D 92, 075014 (2015)
And work in progress with Eibun Senaha

Baldes, T. Konstandin and G. Servant, arXiv:1604.04526,,I. Baldes, T. Konstandin and G. Servant, JHEP 1612, 073 (2016) S. Bruggisser, T. Konstandin and G. Servant, JCAP 1711, no. 11, 034 (2017)

Dynamical CP violation can be produced during first-order phase transition process in the early universe induced by the complex Yukawa coupling.

For example, at temperature around 100 GeV, the new doublet scalar could have a complex VEV during the strong first-order phase transition in some parameter spaces, and then CP violating VEV is transferred to the baryon asymmetry production process through the new lepton Yukawa interaction with the following diagram.

$$\langle\Phi\rangle = \begin{pmatrix} 0 \\ \frac{1}{\sqrt{2}}\varphi \end{pmatrix} = \begin{pmatrix} 0 \\ \frac{1}{\sqrt{2}}\varphi_1 \end{pmatrix}, \quad \langle\eta\rangle = e^{i\theta}\begin{pmatrix} 0 \\ \frac{1}{\sqrt{2}}\varphi_\eta \end{pmatrix} = \begin{pmatrix} 0 \\ \frac{1}{\sqrt{2}}(\varphi_2 + i\varphi_3) \end{pmatrix}$$

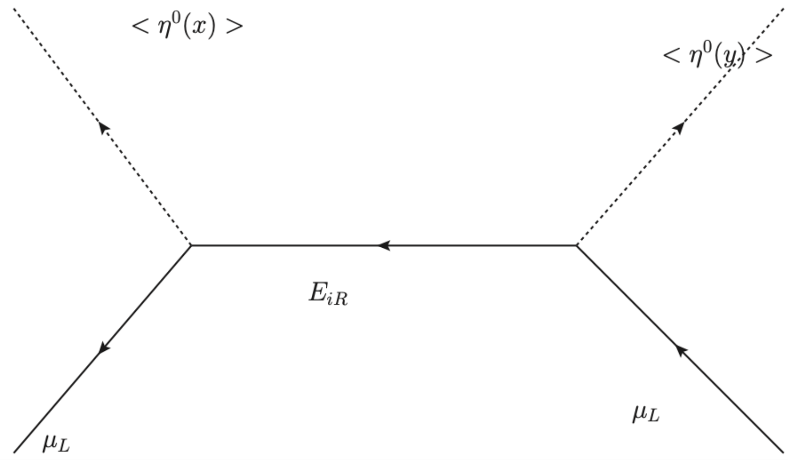

At late time, T=0, the CP violation disappears: $\varphi_1 = v,\ \varphi_2 = \varphi_3 = 0$

Strong First-order EW phase transition

The daisy-improved 1-loop effective potential is

$$V_{\text{eff}}(\boldsymbol{\varphi}) = V_0(\boldsymbol{\varphi}) + V_1(\boldsymbol{\varphi}; T) + V_{\text{daisy}}(\boldsymbol{\varphi}; T), \tag{4.2}$$

where $\boldsymbol{\varphi} = \{\varphi_1, \varphi_2, \varphi_3\}$ and

$$\begin{aligned}
V_0(\boldsymbol{\varphi}) &= \frac{1}{2}\mu_1^2\varphi_1^2 + \frac{1}{2}\mu_2^2(\varphi_2^2+\varphi_3^2) + \frac{\lambda_1}{8}\varphi_1^4 + \frac{\lambda_2}{8}(\varphi_2^2+\varphi_3^2)^2 + \frac{1}{4}(\lambda_3+\lambda_4)\varphi_1^2(\varphi_2^2+\varphi_3^2) \\
&\quad + \frac{1}{4}\Big[R_5\varphi_1^2(\varphi_2^2-\varphi_3^2) - 2I_5\varphi_1^2\varphi_2\varphi_3\Big]
\end{aligned}$$

$$V_1(\boldsymbol{\varphi}; T) = \sum_i n_i \left[V_{\text{CW}}(\bar{m}_i^2) + \frac{T^4}{2\pi^2} I_{B,F}\left(\frac{\bar{m}_i^2}{T^2}\right)\right], \tag{4.3}$$

$$V_{\text{daisy}}(\boldsymbol{\varphi}; T) = -\sum_{\substack{j=h,H,A,H^\pm,G^0,G^\pm,\\ W_L,Z_L,\gamma_L}} n_j \frac{T}{12\pi}\Big[(\bar{M}_j^2)^{3/2} - (\bar{m}_j^2)^{3/2}\Big], \tag{4.4}$$

with $i = h, H, A, H^\pm, G^0, G^\pm, W, Z, t$ and $R_5 = \text{Re}(\lambda_5)$ and $I_5 = \text{Im}(\lambda_5)$. V_{CW} and $I_{B,F}(a^2)$ are defined by

CP-violating source term

Using the Closed-Time-Path (CTP) formalism, the CP-violating source of the SM lepton i induced

by the vector-like lepton j may be cast into the form

$$S_{\ell_i}(X) = \frac{|y_{\ell_i E_j}|^2}{2} v_\eta^2(X)\dot{\theta}(X) H(m_i, \Gamma_i, m_j, \Gamma_j)$$

$$H(m_i, \Gamma_i, m_j, \Gamma_j) = \int_0^\infty \frac{dk\ k^2}{\pi^2} \frac{1}{\omega_i \omega_j} \mathrm{Im}\left[(-1 + n_i + n_j)\frac{\mathcal{E}_i \mathcal{E}_j + k^2}{(\mathcal{E}_i + \mathcal{E}_j)^2} + (-n_i^* + n_j)\frac{\mathcal{E}_i^* \mathcal{E}_j - k^2}{(\mathcal{E}_i^* - \mathcal{E}_j)^2}\right]$$

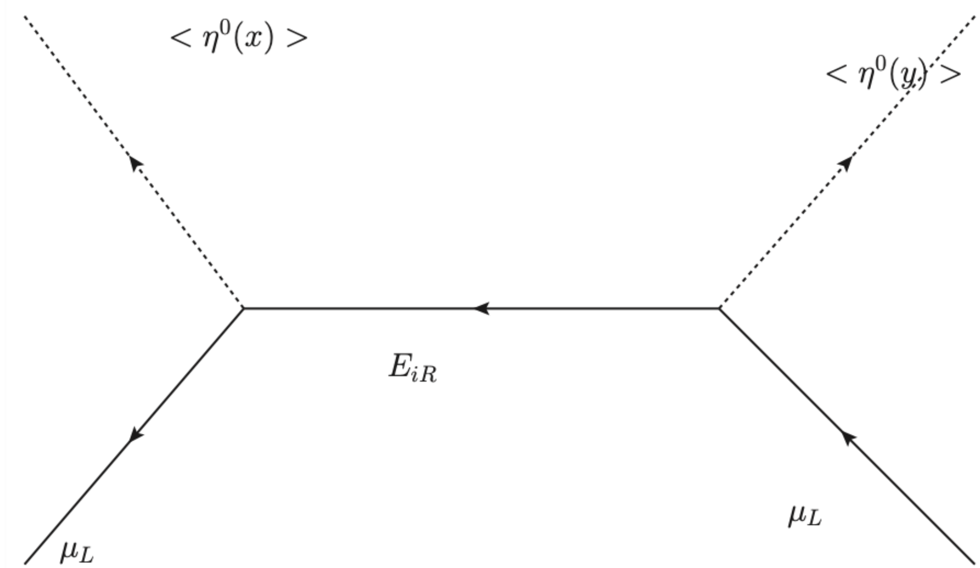

Diffusion equations

The relevant particle number densities are

$$Q_3 = n_{t_L} + n_{b_L}, \quad T = n_{t_R}, \quad B = n_{b_R},$$
$$L_2 = n_{\nu_{\mu_L}} + n_{\mu_L}, \quad E_R = n_{E_R},$$
$$H = n_{\Phi^+} + n_{\Phi^0} + n_{\eta^+} + n_{\eta^0}.$$

The set of Boltzmann equations is given by

$$\begin{aligned}
\partial_\mu j^\mu_{Q_3} &= -\Gamma_{Y_t}(\xi_{Q_3} + \xi_H - \xi_T) + \Gamma_{M_t}(\xi_T - \xi_{Q_3}) - 2\Gamma_{ss} N_5, \\
\partial_\mu j^\mu_{T} &= \Gamma_{Y_t}(\xi_{Q_3} + \xi_H - \xi_T) - \Gamma_{M_t}(\xi_T - \xi_{Q_3}) + \Gamma_{ss} N_5, \\
\partial_\mu j^\mu_{L_2} &= -\Gamma_{Y_{\mu E}}(\xi_{L_2} - \xi_H - \xi_R) + \Gamma^+_{M_{\mu E}}(\xi_{R_2} + \xi_{L_2}) + \Gamma^-_{M_{\mu E}}(\xi_{R_2} - \xi_{L_2}) + S_{\mu_L}, \\
\partial_\mu j^\mu_{E_R} &= \Gamma_{Y_{\mu E}}(\xi_{L_2} - \xi_H - \xi_R) - \Gamma^+_{M_{\mu E}}(\xi_{R_2} + \xi_{L_2}) - \Gamma^-_{M_{\mu E}}(\xi_{R_2} - \xi_{L_2}) - S_{\mu_L}, \\
\partial_\mu j^\mu_{H} &= \Gamma_{Y_t}(\xi_{Q_3} + \xi_H - \xi_T) + \Gamma_{Y_{\mu E}}(\xi_{L_2} - \xi_H - \xi_R) - \Gamma_H \xi_H,
\end{aligned}$$

CP-conserving source term

$$\Gamma_{\ell_i}(X) = \Gamma^+_{\ell_i}(X)(\mu_{E_j} + \mu_{\ell_i}) + \Gamma^-_{\ell_i}(X)(\mu_{E_j} - \mu_{\ell_i})$$

$$\Gamma^\pm_{\ell_i}(X) = \frac{|y_{\ell_i E_j}|^2}{2T} v_\eta^2(X) \int_0^\infty \frac{dk\ k^2}{2\pi^2} \frac{1}{\omega_i \omega_j} \mathrm{Im}\left[(\tilde{n}_j \mp \tilde{n}_i) \frac{\mathcal{E}_j \mathcal{E}_i + k^2}{\mathcal{E}_j + \mathcal{E}_i} + (\tilde{n}_j \mp \tilde{n}_i^*) \frac{\mathcal{E}_j \mathcal{E}_i^* - k^2}{\mathcal{E}_j - \mathcal{E}_i^*} \right]$$

$$D_Q n_B''(\bar{z}) - v_w n_B'(\bar{z}) - \theta(-\bar{z}) \mathcal{R} n_B(\bar{z}) = \theta(-\bar{z}) \frac{N_g}{2} \Gamma_B^{(\mathrm{sym})} n_L(\bar{z})$$

Dark Matter

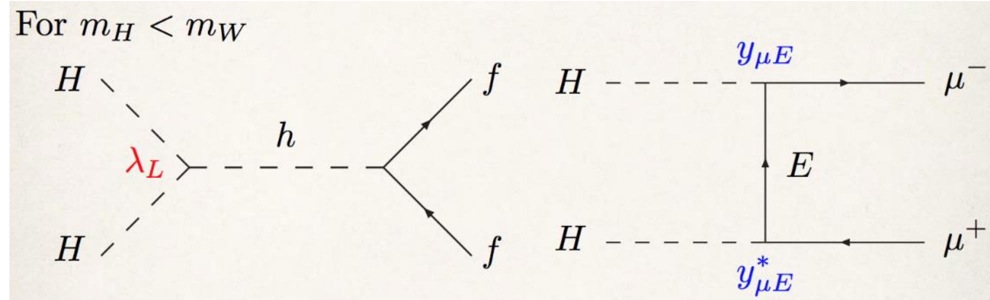

$$m_h^2 = \lambda_1 v^2,$$

$$m_{H^\pm}^2 = \mu_2^2 + \frac{1}{2}\lambda_3 v^2,$$

$$m_H^2 = \mu_2^2 + \frac{1}{2}(\lambda_3 + \lambda_4 + \lambda_5)v^2 = m_{H^\pm}^2 + \frac{1}{2}(\lambda_4 + \lambda_5)\, v^2,$$

$$m_A^2 = \mu_2^2 + \frac{1}{2}(\lambda_3 + \lambda_4 - \lambda_5)v^2 = m_{H^\pm}^2 + \frac{1}{2}(\lambda_4 - \lambda_5)\, v^2,$$

Without loss of generality, we can assume $\lambda_4 + \lambda_5 < 0 \text{ and } \lambda_5 < 0,$

In this simple scenario, the CP-even particle H can be DM candidate.

Further, if $\lambda_4 = \lambda_5 < 0$ **,T parameter is zero and** $m_{H^\pm} = m_A$

Planck 2018

$$\Omega_{\rm DM} h^2 = 0.11933 \pm 0.00091.$$

As for the DM direct detection, the recent XENON1T data put a strong constraint on the DM-nucleon spin-independent elastic scatter cross-section $\sigma_{\rm SI}$. For instance, the most excluded region at 90% confidence level reaches $\sigma_{\rm SI} = 4.1 \times 10^{-47}$ cm^2 with the DM mass of 30 GeV. Therefore, for a light DM, the direct detection data favor the so-called Higgs funnel region where the DM mass is close to half of the Higgs mass, namely, $m_H \simeq m_h/2 \simeq 63$ GeV. In this model, the cross-section $\sigma_{\rm SI}$ is approximated as

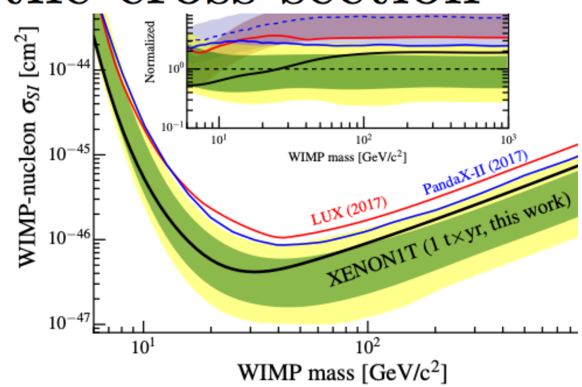

$$\sigma_{\rm SI} \simeq \frac{\lambda_L^2 f_N^2}{4\pi}\left(\frac{m_N^2}{m_H m_h^2}\right)^2$$

where $\lambda_L = \lambda_3 + \lambda_4 + \lambda_5$ and $f_N \simeq 0.3$. To evade the current DM direct detection constraints in this Higgs funnel region, $\lambda_L \lesssim 0.003$ is required

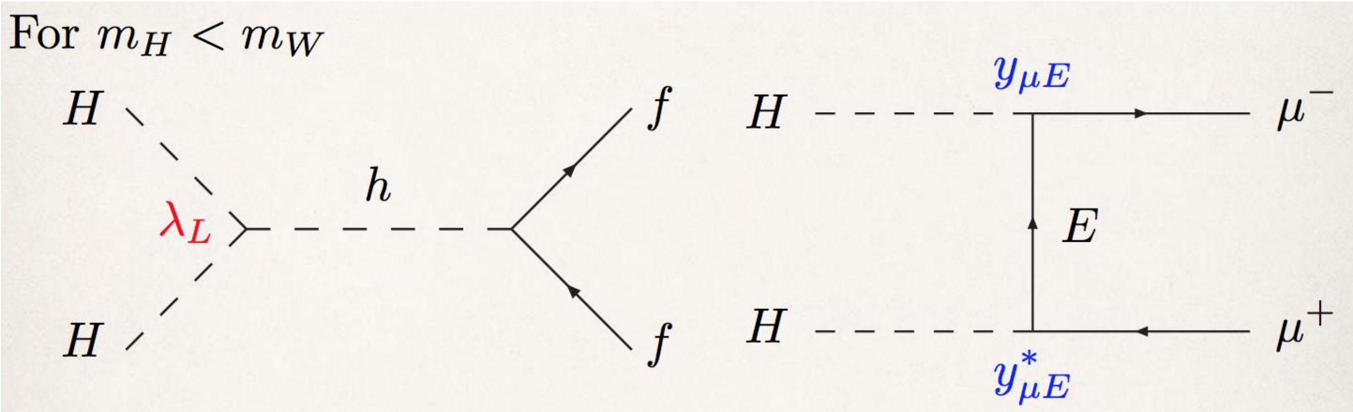

As a benchmark scenario, we consider

$$m_E = (105 - 125)\ \text{GeV}, \quad |y_{\mu E}| = 1.0, 0.5 \text{ and } 0.3.$$

Allowed by LHC data， Lorenzo Calibbi, Robert Ziegler, Jure Zupan, 1804.00009 (JHEP)

The DM relic abundance is always satisfied by judiciously choosing m_H and λ_L. For instance, for $m_E = 110$ GeV and $|y_{\mu E}| = 0.5$, the choice of $m_H = 62.55$ GeV and $\lambda_L = 0.001$ gives $\Omega_{\rm DM} h^2 = 0.12$ and $\sigma_{\rm SI} = 8.7 \times 10^{-48}$ cm^2. Here, we set $m_A = m_{H^\pm} = 300$ GeV and $\lambda_2 = 0.3$, though they are not sensitive to the results.

Direct measurements of vector-like lepton mass

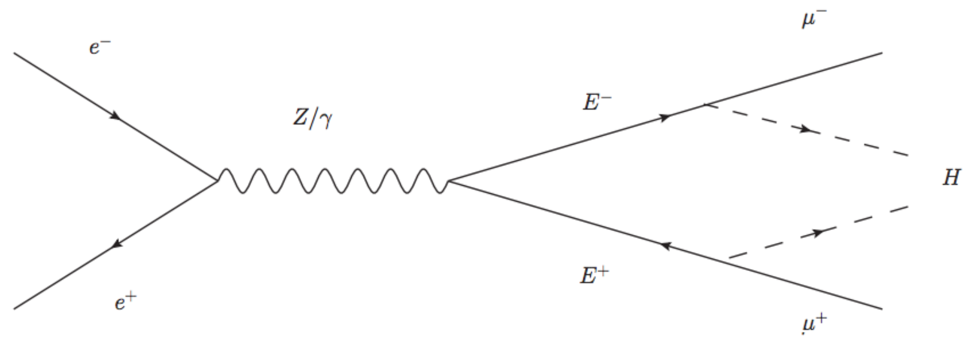

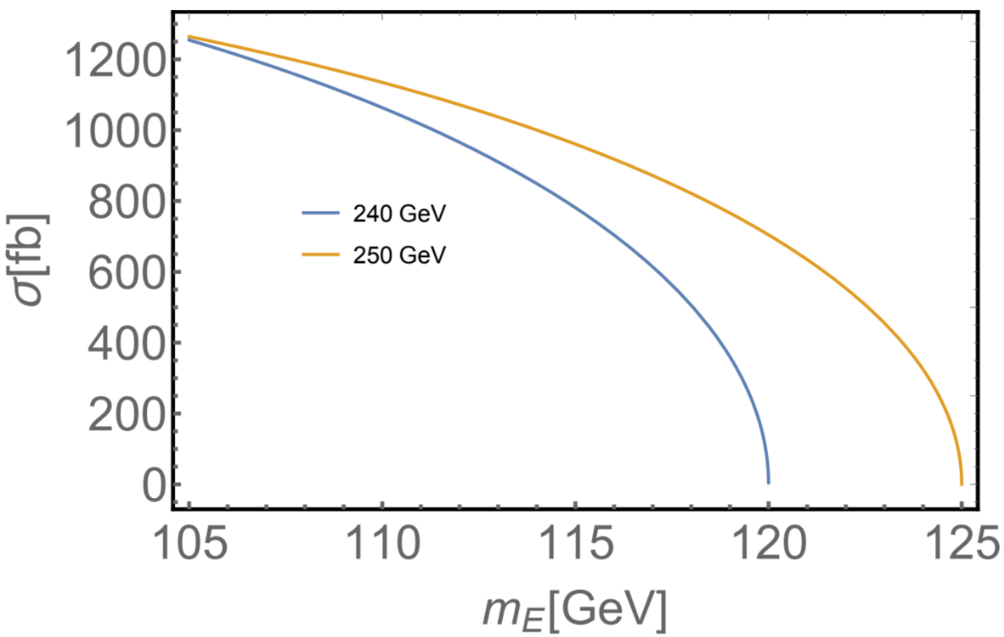

FIG. 6. The cross-section $\sigma(e^+e^- \to \gamma/Z \to E^+E^-)$ as a function of m_E. We take $\sqrt{s} = 240$ GeV (blue) and 250 GeV (orange), respectively.

Indirect search by $Z \to \mu^+\mu^-$

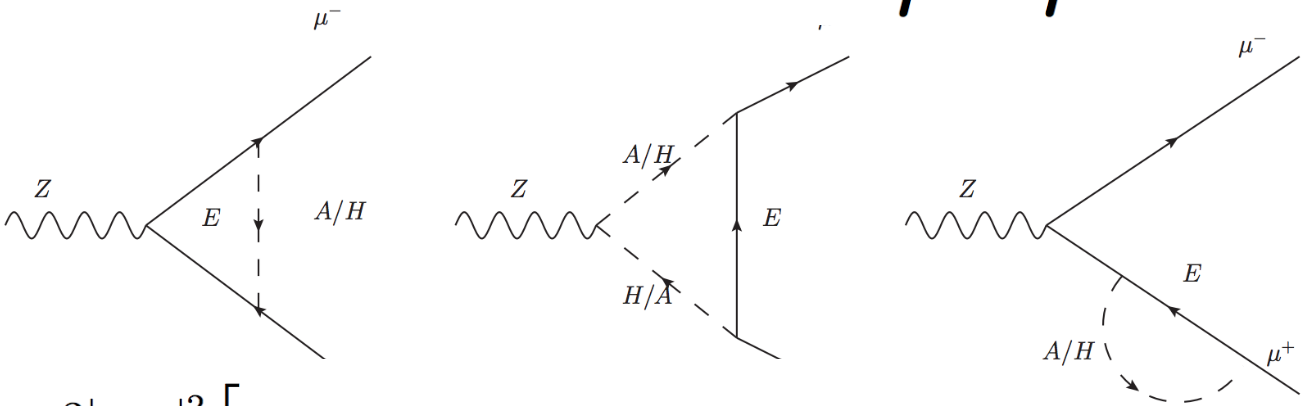

$$\Delta g^L_{Z\bar{\mu}\mu} = \frac{3|y_{\mu E}|^2}{32\pi^2}\Bigg[\tilde{F}_3(m_E, m_H, m_A) + \sum_{\phi=H,A}\Bigg\{\left(-\frac{1}{2}+s_W^2\right)F_2(m_E, m_\phi) + s_W^2 F_3(m_E, m_\phi)\Bigg\}\Bigg]$$

An important missing observable in many previous study!

$$R_{\mu/e} = \frac{\Gamma(Z\to\mu^+\mu^-)}{\Gamma(Z\to e^+e^-)}$$

deviation of $R_{\mu/e}$ from the SM value as

$$\Delta R_{\mu/e} \equiv \frac{R_{\mu/e} - R^{\rm SM}_{\mu/e}}{R^{\rm SM}_{\mu/e}} \simeq \frac{2g^{L,\rm SM}_{Z\bar{\mu}\mu}\mathrm{Re}(\Delta g^L_{Z\bar{\mu}\mu}) + |\Delta g^L_{Z\bar{\mu}\mu}|^2}{|g^{L,\rm SM}_{Z\bar{\mu}\mu}|^2 + |g^{R,\rm SM}_{Z\bar{\mu}\mu}|^2}$$

Large enhancement of Z boson decay by the requirements of EW baryogenesis and DM.

Further generalisation of this enhancement effects from the aspects of symmetry breaking is working in progress.

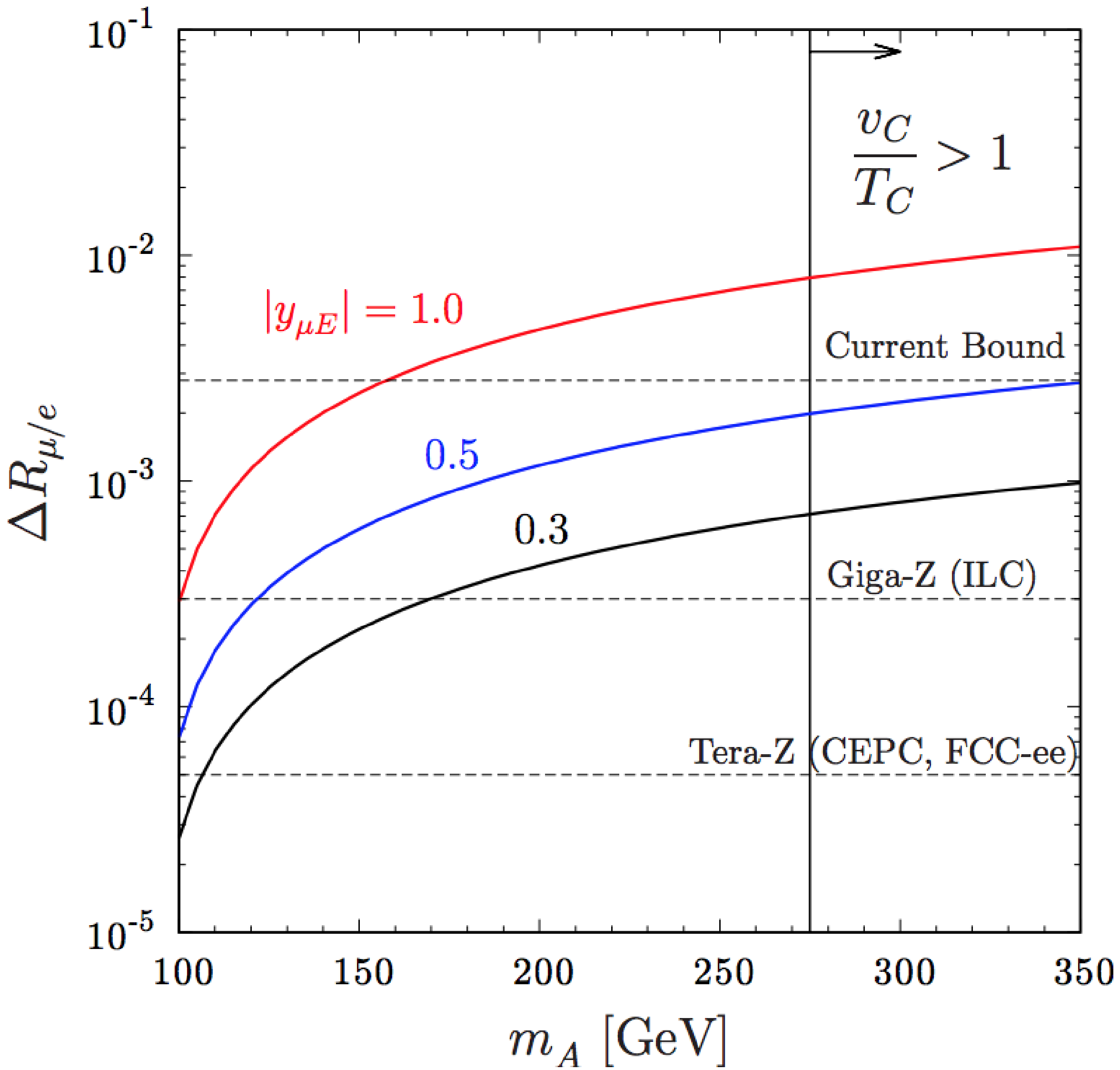

To satisfy the EW strong first-order phase transition (baryogenesis) and DM it requires the large mass splitting of the scalar mass spectrum in the same multiplet, which leads to significant enhancement of the Z boson decay.

Tera-Z can be a new indirect search to explore DM and baryogenesis.

Indirect search by GW signals

Complementary test by GW signals, precise measurements of Z boson decay, HZ cross section measurements and direct production of di-muon plus MET.

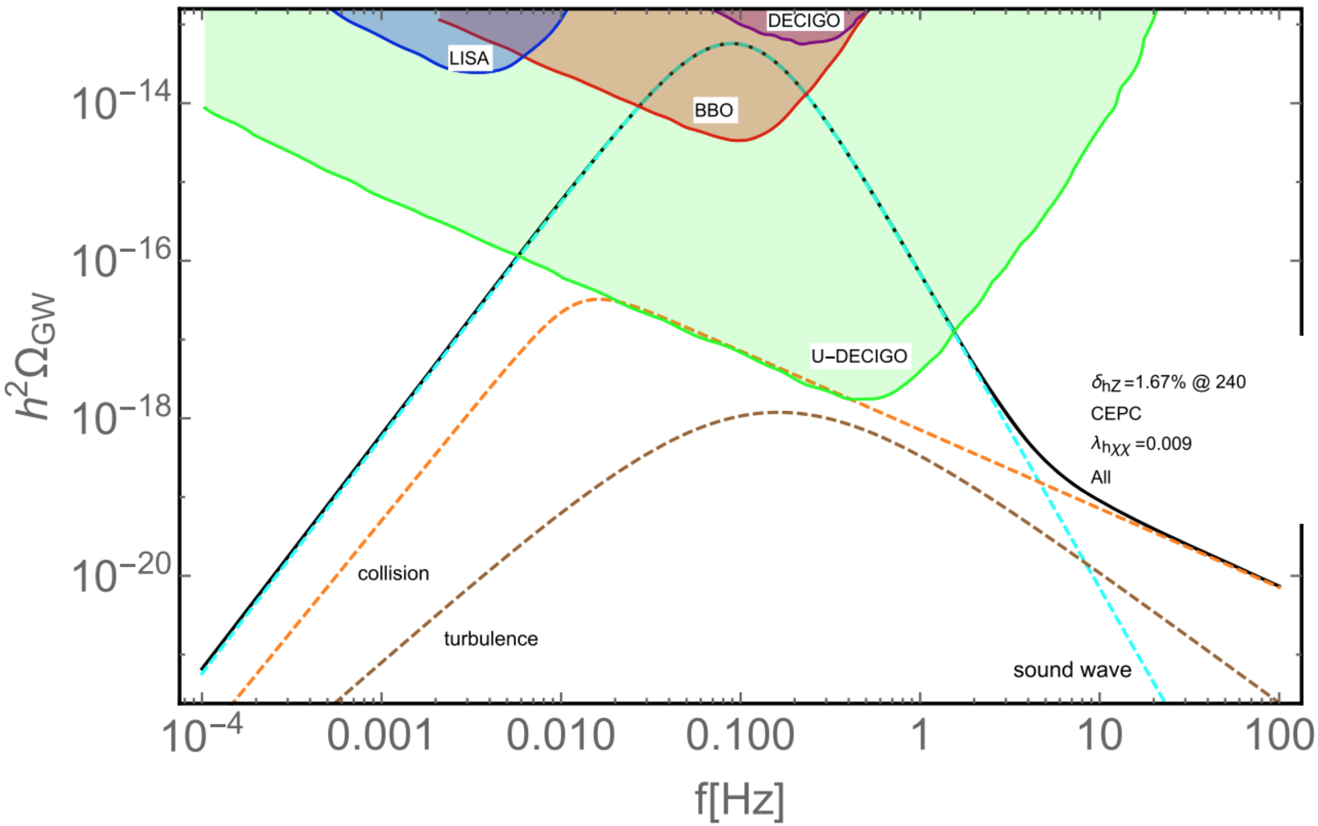

Explore Inert Dark Matter Blind Spots with Gravitational Wave Signatures
FPH,Jiang-Hao Yu,Phys. Rev. D 98, 095022, [2018]

Indirect search by future g-2 precise measurements

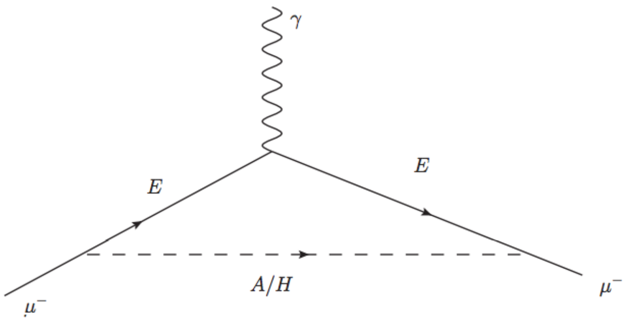

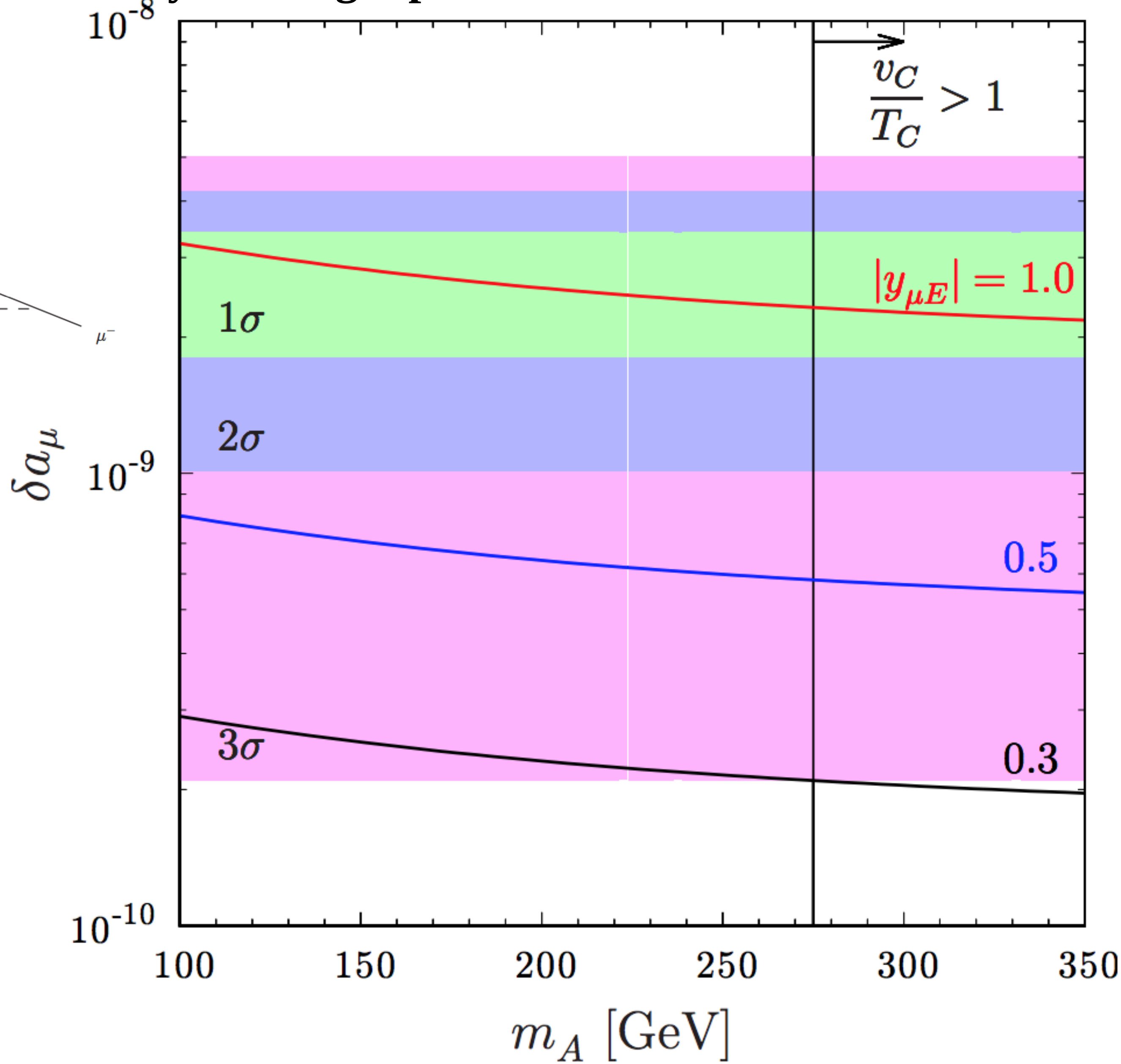

Dynamical CP-violating source

Gravitational wave and collider signals in complex two-Higgs doublet model with dynamical CP-violation at finite temperature
Xiao Wang, FPH, Xinmin Zhang, arXiv: 1909.02978

Dynamical CP-violating source for electroweak baryogenesis can appear only at finite temperature in the complex two-Higgs doublet model, which might help to alleviate the strong constraints from the electric dipole moment experiments. In this scenario, we study the detailed phase transition dynamics and the corresponding gravitational wave signals in synergy with the collider signals at future lepton colliders. For some parameter spaces, various phase transition patterns can occur, such as the multi-step phase transition and supercooling. Gravitational wave in complementary to collider signals can help to pin down the underlying phase transition dynamics or different patterns.

In general

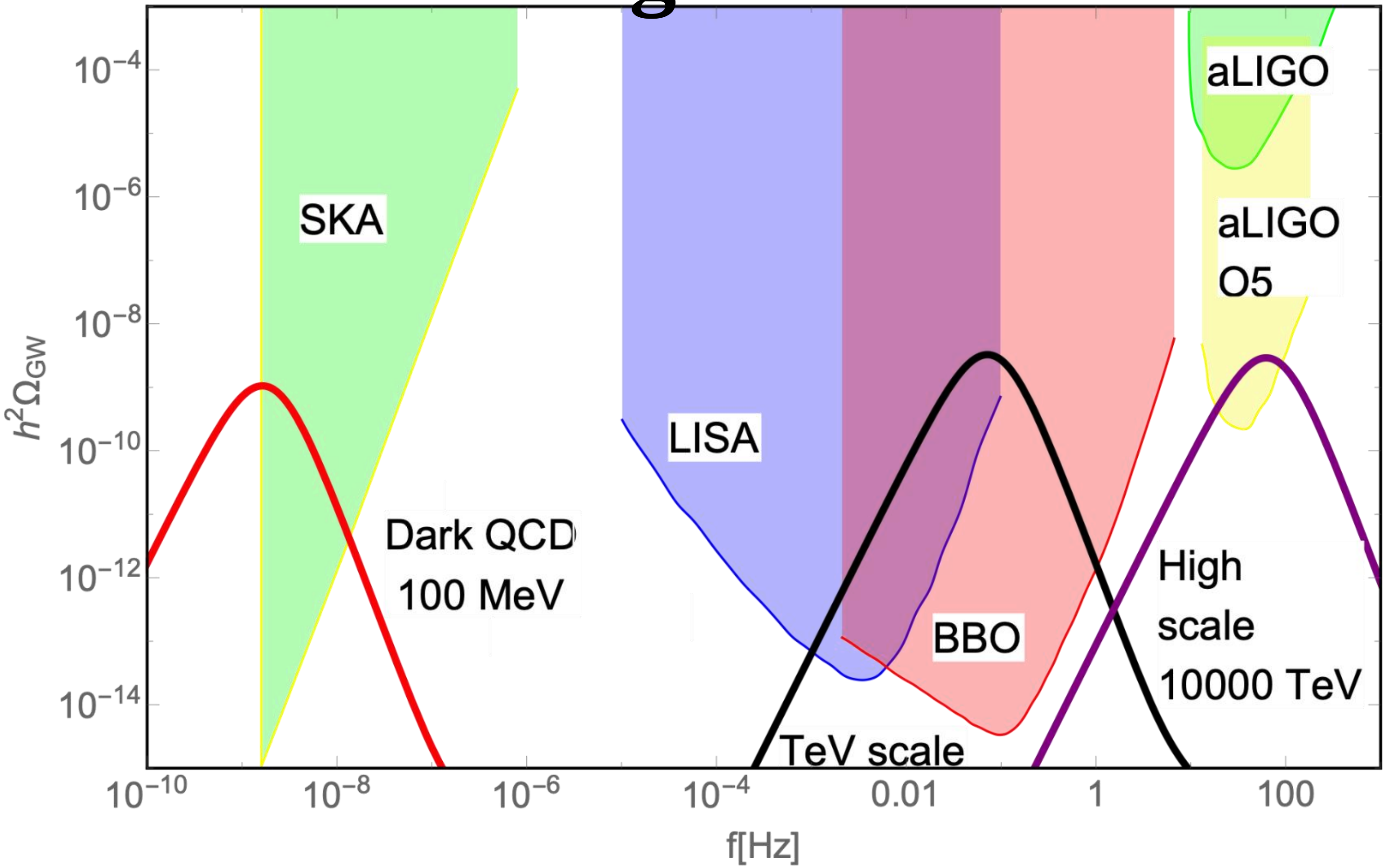

Schematic phase transition GW spectra for SKA-like and LISA-like experiments to explore DM and baryogenesis

FPH, Xinmin Zhang, Physics Letters B 788 (2019) 288-294

arXiv:1905.00891,P. S. Bhupal Dev, F. Ferrer, Y. Zhang, Y. Zhang

arXiv:1602.04203,P. S. Bhupal Dev, A.Mazumdar

Summary and outlook

- **Higgs and axion can provide abundant GW source and radio source ! !**
- **GW becomes a new and realistic approach for new physics**

For example, Probing extra dimension through gravitational wave observations of compact binaries and their electromagnetic counterparts,

H. Yu, B. Gu, **FPH**, Y. Wang , X. Meng， Y. Liu. JCAP 1702 (2017) no.02, 039

The cosmic phase transition with Q-balls production mechanism can explain the baryogenesis and DM simultaneously, where constraints on DM masses and reverse dilution are significantly relaxed. We study how to probe this scenario by collider signals at QCD NLO and GW signals.

FPH, Chong Sheng Li, Phys.Rev. D96 (2017) no.9, 095028

- **The correlation between GW and collider signals can make a double test on the Higgs and scalar dark matter.**
- **SKA-like radio telescopes can provide powerful tools to explore axion dark matter and other fundamental physics.**

Thanks for your attention!

Comments and collaborations are welcome!